January 1981

Design Considerations in the Use of Glauber Salt for Energy Storage

Duane G. Chadwick

Kim H. Sherwood

Design Considerations In The Use Of Glauber Salt For Energy Storage

Duane G. Chadwick
Kim H. Sherwood

Utah Water Research Laboratory
College of Engineering
Utah State University
Logan, Utah 84322

November 1981

WATER RESOURCES PLANNING SERIES
UWRL/P-81/05

DESIGN CONSIDERATIONS IN THE USE OF GLAUBER SALT FOR ENERGY STORAGE

by

Duane G. Chadwick
Kim H. Sherwood

The work on which this report is based was supported in part with funds provided by the Department of Energy

WATER RESOURCES PLANNING SERIES
UWRL/P-81/05

Utah Water Research Laboratory
College of Engineering
Utah State University
Logan, Utah 84322

November 1981

ABSTRACT

Various design concepts for the utilization of the latent heat of Glauber salt at temperatures between 25°C and 50°C were studied. Consideration was given to system economics and what particular heat storage system if perfected would be most cost effective.

The problems of limiting crystal size and heat transfer into and out of salt crystals is discussed. Crystal size is affected by the degree of agitation the salt solution experiences during the salt cooling process. Consequently, crystal size was moderated in a favorable way by introducing air bubbles at the bottom of the salt container. As the bubbles rise a mixing action occurs which limits crystal size and helps prohibit the accumulation of an anhydrous sludge that settles out of solution in the freezing-thawing process.

ACKNOWLEDGMENTS

Acknowledgment is given to the Department of Energy and Utah State University for providing funds to support this project (UEE-151-1).

Appreciation is expressed to Drs. J. Clair Batty, Dean Adams, Melvin Cannon, and Joel E. Fletcher for their assistance and suggestions.

TABLE OF CONTENTS

TABLE OF CONTENTS (CONTINUED)

LIST OF FIGURES

LIST OF FIGURES (CONTINUED)

LIST OF TABLES

INTRODUCTION: ENERGY STORAGE

The utilization of solar radiation as an energy source or space heating, requires two technologies; the solar collector technology for harvesting radiation into the form of thermal energy, and the technology of cost-effective energy storage over long periods of time when no sunshine is available.

Economical energy storage is imperative because space heating needs often are greatest during periods of low incoming radiation and extended durations of fog, and overcast conditions or at night. Much of the economic advantage of solar heating is lost if large investments have to be made for standby heating systems.

Residential space heating represents a large part of the total energy usage in the United States. Roof solar collectors can capture sufficient energy to meet the heating needs for most homes, but suitable low cost thermal energy storage units are needed. Thermal energy can be stored in the specific heat of warm substances or in the latent heat of substances that release energy during phase changes. A promising possibility for heat storage in the temperature range used in space heating is discussed in this report.

LITERATURE REVIEW

Water has a relatively high specific heat and density compared with other compounds or elements. These physical properties coupled with its low cost and high availability, have generated much interest in water as a sensible heat storage media (Sharp and Loehrke 1979, and Hottel and Howard 1971). Hottel and Howard (1971) calculated that 4.5 m^3 of water raised from 38°C to 93°C will supply the equivalent of 10 gal of heating oil burned at 70 percent efficiency, which is a day's heat for a moderately sized dwelling on a cold winter day.

Heat storage in water and other liquids requires sealed tanks and expensive sealed heat exchangers. A solid substances, such as rock, on the other hand, supplies its own heat exchange surface. The specific heat of stone is not very high. A volume of 11.3 m^3 of crushed rock is required to store the same heat as in 4.5 m^3 of water with the same temperature rise (Hottel and Howard 1971).

Scrap iron has a specific heat only half that of stone, but its density is nearly three times as large. One m^3 of iron ore or scrap iron with 30 percent void space must be heated to 371°C to store the same energy as the 4.5 m^3 of water raised from 38°C to 93°C (Hottel and Howard 1971). Because of these factors the cost of heat storage in iron was about 16 fold that of storage in rock (Altman 1971).

In heating, physical or chemical changes may occur, which absorb heat without changing the temperature of the material. When the temperature is reduced, heat is liberated without temperature reduction. The amount of latent heat of these physiochemical reactions for heat energy storage has been extensively studied (Bauerle et al. 1975, Schmidt and Lowe 1976, and Prengle and Sun 1976). In the high temperature range of 200° to over 1000°C a large number of reactions have been identified (Schmidt and Lowe 1976). An interesting scheme has been proposed that reversibly reacts ammonia, water, and sulfur trioxide to form ammonium bisulfate at about 500°C (Prengle and Sun 1976). $Ca(OH)_2$ and $Mg(OH)_2$ can be reversibly dehydrated at about 400°C to CaO and MgO, respectively (Bauerle et al. 1975).

An interesting class of physical reactions, which isothermally store heat, is the melting or fusion reaction. Salt fusion energy storage has been explored over the temperature range 250°C to 350°C (Lefrois et al. 1979). Unfortunately, to obtain these temperatures is quite costly in collector design. The large demand for comfort control heating in the 20°C to 30°C range has spurred particular interest in moderate to low temperature melting materials with commensurate savings possible in collector construction costs (Altman 1971, Telkes 1974, and Lane et al. 1975a, b, c, 1976). Various salt hydrates have attractive heat of fusion characteristics in the 30 to 50°C melting range. Some of their specific characteristics are presented below.

Salt Hydrates

Energy Density

One of the highest latent heats of fusion for commonly available material is that of water. Water releases 335 kJ/kg as it melts from ice. Table 1 gives the latent heat values and densities for several salt hydrates which solidify at temperatures between 20°C and 38°C. The large latent heats of these phase changes are a result of the large quantities of water incorporated in these salt hydrate crystals. In Glaubers salt, for example, there are 10 water molecules for each Na_2SO_4 molecules.

The density information of Table 1 can be used to convert the latent heats into energy densities. Glaubers salt has a theoretical value of 36.7×10^4 kJ/m^3. While some of the other salts may be slightly higher in energy density, the availability of Glaubers salt makes it a likely candidate for study.

Comparison of various economic parameters between various salt compounds is also an important consideration. The best compound, from its physical characteristic standpoint, may be totally impractical if its cost is exorbitant. Table 2 compares the kwatt-hr/$ cost for eight materials possible for use as storage media. Glauber salt is shown to be most cost effective of all that were reported in the table.

Internal Heat Transfer and Incongruent Melting

A problem of obtaining adequate heat transfer arises in using salt hydrates. Since the heat of fusion is only about 12°C above the desired ambient room temperature, there is little temperature gradient available. Pumping large volumes of air over finned surfaces is possible although quite energy intensive.

Table 1. The physical properties of latent heat energy storage materials.

Material Formula	Melting Point °C	Latent Heat kJ/kg	Latent Heat Density kJ/m^3	Thermal Conductivity watts/m°C	References
Glauber Salt $Na_2SO_4 \cdot 10H_2O$	32.2	251	36.7×10^4	0.51	Telkes (1974), Altman (1971) Jurinak and Abdel-Khalik (1978) Washburn (1929)
Thickened Glauber Salt $Na_2SO_4 \cdot 10H_2O + SiO_2$	31.7	126 (May be improved)	18.4×10^4		Telkes (1974) Lane et al. (1975a)
Washing Soda $Na_2CO_3 \cdot 10H_2O$	32.2-33.9	247-251	35.6×10^4 to 36.1×10^4		Telkes (1974) Altman (1971) Lane et al. (1975a)
Calcium Chloride $CaCl_2 \cdot 6H_2O$	28.9-29.4	170-183	29.1×10^4 31.3×10^4	Solid 1.09 Liquid 0.54	Telkes (1974) Altman (1971) Lane et al. (1975a)
Sodium Phosphate $Na_2HPO_4 \cdot 12H_2O$	36.1	265	40.3×10^4		Telkes (1974) Altman (1971) Lane et al. (1975a)
Sodium Thiosulfate $Na_2S_2O_3 \cdot 5H_2O$	47.8-48.9	209	32.1×10^4	0.57	Telkes (1974), Altman (1971) Lane et al. (1975a) Lorsch (1974)
Barium Hydroxide $Ba(OH)_2 \cdot 8H_2O$	77.8	279-305	60.8×10^4 66.5×10^4	Solid 1.26 Liquid 0.65	Telkes (1974), Altman (1971) Lane et al. (1975a)
Sunoco P116 Paraffin $(CH_2)_n$	46.7	209	19.3×10^4	Solid 0.14 Liquid 0.15	Jurinak and Abdel-Khalik (1978) Lorsch (1974)

Table 2. The economic parameters of latent heat energy storage materials.

Material Formula	Melting Point °C	Latent Heat Density kJ/m^3	Material Cost, K[a] $/100 kg	Value of Material for Energy Storage K_2 = $0.0/m^3 kWatt Hr/$	K_2 = $100/m^3 kWatt Hr/$	K_2 = $200/m^3 kWatt Hr/$	References
Glauber Salt $Na_2SO_4 \cdot 10H_2O$	32.2	3.67×10^5	5.04	1.38	0.500	0.306	Telkes (1974), Altman (1971) Jurinak and Abdel-Khalik (1978) Washburn (1929)
Thickened Glauber Salt $Na_2SO_4 \cdot 10H_2O + SiO_2$	31.7	1.84×10^5	5.27	0.664	0.247	0.152	Telkes (1974) Lane et al. (1975a)
Washing Soda $Na_2CO_3 \cdot 10H_2O$	32.2-33.9	3.56×10^5 to 3.61×10^5	10.08	0.692	0.362	0.245	Telkes (1974), Altman (1971) Lane et al. (1975a)
Calcium Chloride $CaCl_2 \cdot 6H_2O$	28.9-29.4	2.91×10^5 to 3.13×10^5	7.56	0.672	0.335	0.223	Telkes (1974), Altman (1971) Lane et al. (1975a)
Sodium Phosphate $Na_2HPO_4 \cdot 12H_2O$	36.1	4.03×10^5	22.67	0.325	0.236	0.185	Telkes (1974), Altman (1971) Lane et al. (1975a)
Sodium Thiosulfate $Na_2S_2O_3 \cdot 5H_2O$	47.8-48.9	3.21×10^5	36.41	0.159	0.129	0.109	Telkes (1974), Altman (1971) Lane et al. (1975a) Lorsch (1974)
Barium Hydroxide $Ba(OH)_2 \cdot 8H_2O$	77.8	6.08×10^5 to 6.65×10^5	63.20	0.134	0.122	0.113	Telkes (1974), Altman (1971) Lane et al. (1975a)
Sunoco P116 Paraffin $(CH_2)_n$	46.7	1.93×10^5	43.51	0.133	0.101	0.081	Jurinak and Abdel-Khalik (1978) Lorsch (1974)

[a]1971 prices from Altman (1971) updated to February 1980 by 129 percent increase from Monthly Labor Review (March 1972 to February 1980) (Chemical and Allied Products Cost Index) (U.S. Dept. of Labor 1980).

In contrast to the economics of forced air convection, pumped water convection is much more economical. Pumping a semi-frozen material (while absorbing or releasing latent heat through a phase change), however, presents several mechanical problems. An additional problem exists in that most hydrated salts do not melt congruently, but rather "decompose" into a saturated solution and a less hydrated insoluble fraction (Telkes 1974, Mills et al. 1979, and Lane et al. 1975a).

Findlay (1945) presents an extensive discussion of the thermodynamics of the incongruent melting of Glauber salt ($Na_2SO_4 \cdot 10H_2O$). At 32.6°C a quadruple point of stability is reached for anhydrous sodium sulfate, sodium sulfate decahydrate, and a solution saturated with respect to both of these salts. Either stirring or thickening allows for fairly complete reversibility of these types of melting phenomena (Hottel and Howard 1971, Telkes 1974, Lane et al. 1975a, b, c, and Mills et al. 1979).

Three basic mechanical stirring techniques have been studied: blade type stirring (Lefrois et al. 1979), rotation of drums (Herrick and Thornton 1979), and oil recirculation (Mills et al. 1979). A one-quarter horsepower motor can mix a 55 gallon drum of Glauber salt ($Na_2SO_4 \cdot 10H_2O$) by rolling it along its longitudinal axis. By the convection heat transfer process it has a heat transfer coefficient of between 568 and 57 watts/m^2 °C depending on the degree of solidification of the material in the drum (Herrick and Thornton 1979). Oil recirculation through Glaubers salt is characterized by salt carry-over problems (Mills et al. 1979). A less attractive alternative is proposed involving dilution of eutectic mixtures to allow continuous stirring. A rather expensive eutectic mixture consisting of potassium fluoride, ethylene glycol, and water which stores 142 kJ/kg has been proposed (Keller 1978). By roughly doubling the volume of Glauber salt with water, complete melting can be achieved (Biswas 1977).

While thickening hydrated salts to prevent separation eliminates the requirement for internal mixing, it also eliminates internal convective heat transfer. This leaves only conductive heat transfer to move heat to the surface for distribution and use. The thermal conductivity of unmodified Glauber salt ($Na_2SO_4 \cdot 10H_2O$) has been determined to be 0.51 watts/m^2 °C (Jurinak and Abdel-Khalik 1978). Tables 1 and 2 include this information as well as other thermal conductivity data. Table 2 shows the extremely poor thermal conductivity and high cost of Sunoco P116 paraffin wax (Keller 1978, Jurinak and Abdel-Khalik 1978, and Lorsch 1974). With thickened material the thermal conductivity is very likely to be most influenced by the continuous part of the mixture. For this reason, adding highly conductive material like metal chips is not effective in increasing the thermal conductivity of latent heat storage materials.

Lane et al. (1975a) have experimented with encapsulating $CaCl_2 \cdot 6H_2O$ in aluminum foam. Under these conditions, a continuously connected aluminum matrix, similar to the continuous foils used by Colloidal Materials (1979) allows a low temperature to be maintained in the heart of a rather large package of latent heat storage material. Since the thickening agent is relatively fluid, this part of a thickened media is most likely continuous around the solid crystals. A nomograph for estimating thermal conductivity of two phase systems is presented by Ratcliffe (1968) (see Appendix A).

When confined to conductive internal heat transfer, the thickness of the conducting material becomes a primary consideration. If the thermal resistance in a body is small compared to the heat transfer at the surface of the body, heat transport will be controlled by external convection only. This type of heat transfer is referred to as "lumped heat." This type of analysis is good when the Biot modulus (the ratio of the external heat transfer coefficient times a characteristic length to the thermal conductivity of the body) is less than 0.1 (Holman 1972, Obert and Young 1962). For cylindrical symmetry the characteristic length is the ratio of the volume to the area:

$$h\ell/k_s \leq 0.1 \quad \text{with } \ell = r/2 \quad . \quad . \quad . \quad . \quad . \quad (1)$$

$$hr/2k_s \leq 0.1 \quad . \quad . \quad . \quad . \quad . \quad . \quad . \quad . \quad . \quad (2)$$

where

h = external heat transfer coefficient (E/L^2Tt)

ℓ = characteristic length, the radius of the cylinder divided by 2 (L)

k_s = thermal conductivity of the body (E/LTt)

A critical container radius also exists for any particular thermal conductivity and convective environment, which will produce a maximum heat exchange per unit length (Obert and Young 1962). This critical radius (r_{crit}) is given by:

$$r_{crit} = k_s/h \quad . \quad . \quad . \quad . \quad . \quad . \quad . \quad . \quad . \quad (3)$$

where k_s and h are as defined before, the thermal conductivty and the heat transfer coefficient, respectively. While this critical radius is derived from a steady state assumption, materials with large latent heats of crystallization lead to nearly steady state temperature profiles in the solidified material. The complexity of heat conduction with a phase change has lead to chemical diffusion analog procedures for modeling purposes (Hashemi and Sliepcevich 1967). Under the assumption of an approximately steady state temperature profile, in the solid material an analytical solution is possible. The general partial differential equation for cylindrical symmetry (Figure 1):

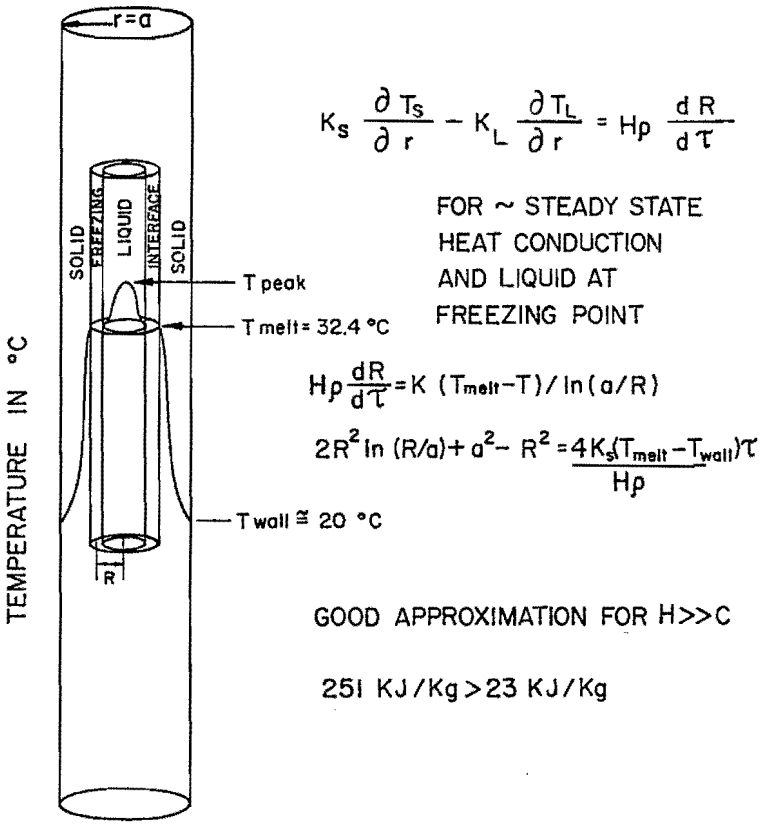

Figure 1. A theoretical temperature profile for a cylindrically freezing liquid.

$$k_s \, \partial T/\partial r - k_l \, \partial T/\partial r = H\rho dR/d\tau \quad . \quad . \quad . \quad . \quad (4)$$

becomes:

$$dR/d\tau = (k_s/H\rho)(T_{melt} - T_{exit})(R\ell n(a/r)) \quad . \quad . \quad . \quad (5)$$

under the steady state temperature profile assumption. Equation 32 integrates to give:

$$4k_s\tau(T_{melt} - T_{exit})H\rho = 2R^2\ell n(R/a) - R^2 + a^2 \quad . \quad . \quad (6)$$

where

k_s = thermal conductivity of the solid (E/LTt)

τ = time from initiation of freezing (t)

T_{melt} = melting temperature of the material (T)

T_{exit} = temperature maintained at the outside of the freezing cylinder (T)

H = latent heat of fusion per unit mass (E/M)

ρ = density (M/L^3)

As the time advances the radius remaining fluid, R, changes as shown, where a is the radius of the tube containing the fluid (Figure 1) (Carslaw and Jaeger 1959).

Heat Generation

Chemical kinetics may limit the rate of crystallization of some latent heat storage materials. The heat generating step in the solidification of a salt is crystallization from the liquid phase. A wealth of literature exists on crystal growth. Of particular interest in this study is crystallization of salt hydrates from solution and crystallization in gels.

Henisch (1970) studied crystal growth in gels including Cab-O-Sil. For many salts including sodium oxalate and calcium tartrate, the radius (r) of nearly spherical crystals increases proportionally to the square root of the elapsed time (τ).

$$r^2 = C_1\tau \quad . \quad . \quad . \quad . \quad . \quad . \quad . \quad . \quad . \quad (7)$$

In terms of heat generation this means:

$$r^3 \propto Q = C_2\tau^{3/2} \quad . \quad . \quad . \quad . \quad . \quad . \quad . \quad (8)$$

where Q is the total heat released, which is recognized proportional to the cube of the radius (r). If C_2 is large enough this heat flow rate will not be the factor that limits overall heat transfer. This significant liberation of heat should insure that kinetic limitations only occur for a short initial period when crystal size is extremely small.

Montillion and Badger (1927) studied crystal growth of Glauber salt in aqueous solutions. The kinetics of weight deposition onto the existing crystal surface follow the relationship:

$$dW/dS = C_3 e^{C_4 \tau} \quad . \ . \ . \ . \ . \ . \ . \ . \quad (9)$$

where

dW/dS = change of crystal weight with change in surface area (M/L^2)

τ = elapsed time (t)

C_3, C_4 = appropriate constants with complimentary units

The value of C_3 was found to increase from 12.57 kg/cm^2 at 27.1°C to a value of 16.26 kg/cm^2 at 30.9°C. These values look extreme until one observes the time required to bring C_4 with a value of 0.0178/min up to a reasonable exponent for e.

Both of these reports indicate the importance of crystal surface area for the rapid release of heat. If surface area is small, as it most certainly is when crystallization first begins, heat generation is slow. As a result of this small initial crystal growth, melts of many salt hydrates and eutectics cool significantly below the melting point before the crystal growth rate releases significant heat. Supercooling has been observed in a large array of salt hydrates (Telkes 1974 and Lane et al. 1975a). Among those salts exhibiting supercooling are $CaCl_2 \cdot 6H_2O$, $Na_2HPO_4 \cdot 12H_2O$, $Ca(NO_3)_2 \cdot nH_2O$, and $Na_2SO_4 \cdot 10H_2O$ (Telkes 1974). Nucleating agents, which greatly reduce this tendency to supercool, have been identified for all these salt hydrates. Telkes (1974) and Johnson (1977) both report excellent crystal seeding of Glauber salt ($Na_2SO_4 \cdot 10H_2O$) with about 3 to 4 percent of the nearly perfectly isomorphous crystals of borax ($Na_2B_4O_7 \cdot 10H_2O$). Seeding Glauber salt reduces the melting temperature to about 31.7°C (Telkes 1974). It appears that chemical kinetics do not limit salt hydrate energy recovery.

Conclusions from the Literature Review

In concluding the literature review several observations can be made. 1) Several salts identified in Tables 1 and 2 have large heat storage coefficients at temperatures above the ambient room temperature. 2) There is a tendency for separation of the water molecule from the parent compound leaving an anhydrous salt which becomes relatively useless for storing heat. 3) Three ways are reported in the literature that are used to try to overcome the decompositon of hydrated salts into an anhydrous material. 4) Heat flow through a non-fluidized crystalline salt is too slow to be very useful for residential heating.

One method used to overcome the formation of anhydrous salts during the heating and cooling cycling process is to use a rolling drum approach which is roughly analogous to a truck mounted concrete mixer. The slight agitation caused by the rolling drum is sufficient to keep the anhydrous material suspended in the solutions long enough to greatly enhance the water-salt combination. A second method is to use a paddle-like stirring mechanism. The third method reported in the literature entails the process of injecting oil at the bottom of the salt solution container. The oil is heated (or cooled) as it rises to the top of the salt container where it is drawn off and circulated through a heat exchanger. Oil, lighter than Glaubers salt, tends to keep the anhydrous material stirred as it floats to the top of the mixture. Literature surveys report serious problems with this method, however.

The rolling drum requires an expensive type of construction to carry the large salt load which can easily amount to several tons. This heavy load may cause drum-wall metal fatigue and ultimate wall failure to occur. Paddle stirring of the salt exhibits profuse crystal growth on the surface of the paddles, limiting their effectiveness. Reports indicate that the oil injection method invariable plugs the recirculation plumbing due to crystal carry over and subsequent accumulation in the oil lines. Another observation from the literature is that if the crystals are adequately fluidized and stirred, heat can be absorbed at a rate that will be limited to the heat transfer rate through the container wall and not due to inadequate crystal growth rates. This is true except for very tiny crystal sizes. Some super cooling is expected to occur as a result when salt freezing first begins and the crystal size is small.

Based on the literature review it appears that an alternative method of storing energy in Glaubers salt should be investigated. Before doing so, however, several investigative processes should be undertaken such as the evaluation of the effects of thixotropic agents on the thermal conductivity, and crystal growth and its effect on reducing the amount of anhydrous sludge that accumulates. The next section discusses some of these experiments and procedures.

MATERIALS AND METHODS

Glauber Salt Preparations

Glauber Salt

"Solar Salts" were obtained from Cabot Corporation's Billerica Technical Center, Billerica, MA 01821. This material was analyzed by standard water analysis techniques and found to contain Na^+, $SO_4^=$, SiO_2, $B_4O_7^=$, and Cl^- (APHA 1975).

A sample of Cabot Corporation's Grade PTG (Lot IG258) amorphous fumed silica (SiO_2) Cab-O-Sil™ was also provided. Experimentation was carried out on both Cabot "Solar Salts" and Cab-O-Sil thickened Glauber salt.

Penick Ford Limited (a subsidiary of Univar, Box 428, Cedar Rapids, IA 52406) supplied 2.27 kg of each of Astro Gum 21 and Astro Gum 3010. These starch gels are modified corn starch, which has been oxidized to carboxy-methyl-amylose.

Great Salt Lake Mineral Co. offered free access to their stockpiles of Glauber salt ($Na_2SO_4.10H_2O$). Three five gallon (5 x 3.785 ℓ) cans of this material were initially obtained. Subsequently, another 500 kg of salt was acquired. "Baker analyzed" reagent grade borax ($Na_2B_4O_7 \cdot 10H_2O$) was used as crystal seed in preparations made from this Glauber salt.

Thickened Glauber salt was prepared with the same general formulation reported by Johnson (1977). No salt (NaCl) or surfactants were used, however. Johnson's formulation calls for 4 g of Cab-O-Sil (SiO_2) and 3 g of borax ($Na_2B_4O_7 \cdot 10H_2O$) per every 100 g liquefied Glauber salt ($Na_2SO_4 \cdot 10H_2O$) that is to be thickened. The first 100 g of thickened Glauber salt prepared was recrystallized from Great Salt Lake Mineral Co. Glauber salt. All subsequent preparations were made directly from material from the stockpiles. No apparent differences were observed with recrystallized material, and recrystallization is not expected to be necessary prior to manufacturing thickened Glauber salt suspensions.

The preparation procedure was initiated by weighing the Glauber salt to be thickened on a balance. The Glauber salt was then warmed slowly to ~ 38°C by which time it had completely decomposed into anhydrous Na_2SO_4 and saturated Na_2SO_4 solution. Borax ($Na_2B_4O_7 \cdot 10H_2O$ 3 g/100 g) and Cab-O-Sil (SiO_2 4 g/100 g) were then added, and the mass was stirred at high speed with a magnetic stirring bar for at least 20 minutes. All preparations were exposed to at least two complete thawing-freezing cycles before any experimentation was attempted.

Starch Gels

Autoclaving a 2.5 percent by weight suspension of either Astro Gum product produced a very thick carboxy-methyl-amylose gel. Any addition of liquified Glauber salt, however, always resulted in coagulation of the gel. Pancreatic amylose did not remove the iodine reaction nor did it generate a more soluble starch derivative. It was hypothesized that this enzyme was rendered ineffective by stearic hindrance caused by the large carboxyl group on the molecule.

Soluble potato starch could not be kept in solution with saturated Na_2SO_4 either. Maltose could be heated into solutions saturated with Na_2SO_4, but the release of water prevented thixotrophy above the decomposition temperature of the Glauber salt.

Thermal Conductivity Measurements

Initially consideration was given to storing salt in long weiner-like plastic tubes. These tubes were conceived to be more than a meter in length and lie submerged in the heat exchange fluid. As a result of this concept a study of the thermal conductivity of salt mounted in thin wall polypropylene was made.

Thermal Conductivity Tubes

Thermal conductivity was measured by the annulus method mentioned by Holman (1966). The thermal conductivity chamber consisted of two lengths of copper pipe. Wall thickness was 0.002 m with the smaller 2.54 cm inside diameter copper tube about 2 cm shorter than the larger 5.04 cm inside diameter copper tube. The smaller-shorter tube was sealed by soldering a copper plate at one end. This narrower sealed tube was then centered in the larger tube with the open end of the smaller tube flush with one end of the larger outside tube. Urethane foam was then placed around the sealed end of the smaller tube inside the larger tube up about 2.5 cm around the smaller inside tube. When the excess foam

was cut off the filled end of the larger tube, this produced an annular region bounded on the outside by the 5.04 cm copper tube, and on the inside by the 2.54 cm copper tube, and on the bottom by urethane foam (Figure 2). The urethane foam served the purpose of keeping the inside copper tube suspended and centered in the outside tube and insulating the lower end of the 2.54 cm tube from contact with anything, either outside tube or table top, with at least 1 cm of urethane foam (thermal conductivity ~0.0003 watts/m C).

A copper-constantan thermocouple was soldered about half way up the outside tube on the outside of the copper tube, and another identical thermocouple was soldered to the inside of the inside copper tube about half way down the inside tube, approximately level with the outside thermocouple. (See Figure 2.)

The inside tube was then filled with N-butanol (water was used initially, but proved overly corrosive). In this temperature bath a 100 ohm resistor was placed and the leads of this resistor were connected to any of a number of regulated DC power supplies. The annulus between the two tubes was filled with a known depth of the material to be tested and a styrofoam cap was pressed down on the top of the two copper pipes to seal the top surfaces of the N-butanol and test material. No attempt was ever made to control the temperature external to the outside copper tube. Free convection in room temperature air was the only heat loss of any significance available for ultimately sinking the heat generated in the 100 ohm resistor.

The power dissipated in the resistor was quantified by measuring the voltage applied

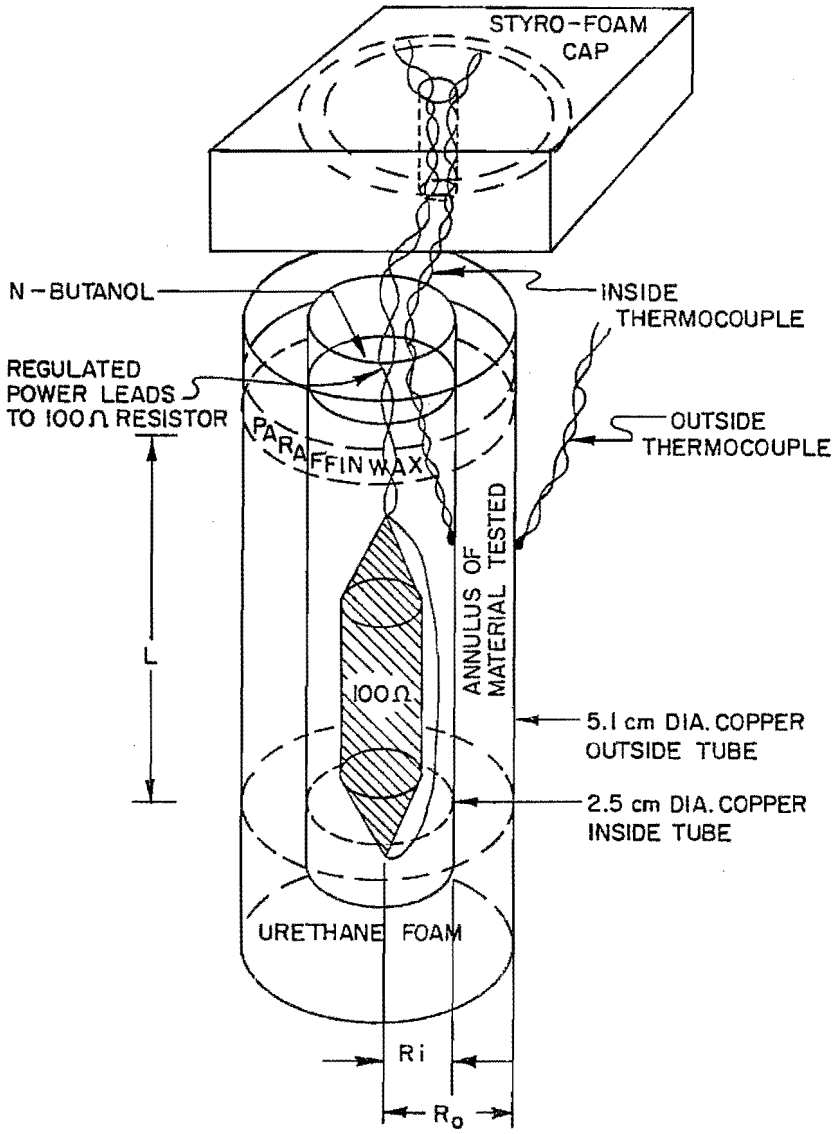

Figure 2. Annular sample thermal conductivity apparatus. Note: Symbols defined in Appendix B.

across the resistor and the electric current flowing through the 100 ohm resistor. This power was assumed to be nearly completely conducted from the inside tube to the outside tube by the material filling the annular region between the two tubes. The temperature difference causing this heat conduction (or in the case of completely fluidized non-thixotropic liquids heat convection) was measured by measuring the temperature of the internal copper tube and the exterior copper tube. The N-butanol was added to prevent hot spots and distribute the heat from the resistor uniformly over the inner surface of the interior copper tube.

Temperature Recording

The temperatures of the inside and outside tube were recorded continuously on a strip chart recorder connected to the two thermocouples. At first, a 12 channel thermocouple recorder was used; however, due to equipment scheduling overlaps, a Rustrak™ two channel recorder was ultimately used. The two channel recorder required referencing both thermocouple circuits to a thermocouple held at ice water temperature (0°C) and required careful setting of the zeroing and attenuation on both channels of this recorder (see Figure 3).

High variance and poor reproducibility in the first week's data prompted the construction of another longer thermal conductivity tube. The failure of this equipment to produce better results coupled with the discovery of some small amount of drift in the two channel recorder, lead to the reuse of the 12 channel recorder. This equipment improvement, however, failed to improve the results. A calibration of the equipment made on Amoco-Parowax™ paraffin, revealed excellent reproducibility with very small variances even with the shortest thermal conductivity tube operating in conjunction with the two channel recorder and the associated ice bath reference. The high variance in the thermal conductivity of the non-homogeneous materials tested was probably a result of variable, history-dependent thermal conductivity of the material itself (see Appendix A).

The thermal conductivity of the test material was calculated by the formula given by Holman (1966):

$$k_s = q\ell n(r_o/r_i)/2\pi L(T_i-T_o) \quad . \quad . \quad . \quad . \quad . \quad (10)$$

where

k_s = thermal conductivity of the material (E/LTt)

q = heat passing through the annulus per unit time (E/t)

r_o/r_i = ratio of the outside radius to the inside radius of the annulus

L = length of material in the annulus (L)

T_i-T_o = temperature difference between the inside and the outside of the annulus of material (T)

The temperatures were taken from the strip chart after at least a 4 hour stabilization period for each given power input q to assure steady state heat transfer. Steady state was verified numerous times by extended constant power periods, some of which lasted for 2 days.

Thin Film Polyethylene Packaging

Packaging

Three sizes of polyethylene tubes were studied. These tubes were sealed twice on both sides in an E-Z™ food bag sealer. Attempts at larger containers sealed with a soldering iron with aluminum foil used to prevent sticking to the soldering iron produced inferior containers. These tubes were made from 2.75 mil thickness NASCO Whirl-lock bags.™ The tubes were approximately 18 cm long and were filled with material prior to sealing the last end of the tube. Tubes 0.4 cm, 1.2 cm, and 2.2 cm in diameter were studied.

Calorimetric Testing

Tubes were tested for heat uptake and release in a 70 mm by 340 mm one liter capacity aluminum shielded Dewar flask. For melting experiments, 500 ml of water was placed in the Dewar flask and for freezing experiments (with the exception of one run on 1.2 cm tubes at 22.2°C) 750 ml of water was required in order to allow the thermometer to protrude sufficiently for measurements to be made. Stirring was found to be necessary. A toy boat motor operating on a size AA 1.5 volt dry cell battery provided adequate mixing within the flask. The power dissipated by the toy boat motor was shown to be an insignificant contribution to the heating of the water in the Dewar flask. The cooling of the flask by itself was studied twice over nearly day long periods. Water was shown to cool exponentially in the Dewar flask towards room temperature with an exponentiation constant of 0.029/hour and a coefficient of determination of 0.9999 (R-SQ). This Dewar flask was fitted with a 65 mm x 80 mm tapered styrofoam stopper 51 mm thick, through which the thermometer and a small 2 mm diameter steel rod were inserted into the Dewar flask. The toy boat motor was fixed on the steel rod. The thermometer was marked from -1.0°C to 101.0°C at 0.1°C intervals. This was a precision mercury thermometer with nitrogen above the mercury (Figure 4).

The tubes of eutectic material studied in this calorimetric apparatus were 0.4 cm, 1.2 cm, and 2.2 cm in diameter and about 18 cm in length. To attempt to maintain similar exposed areas in an experimental run, four of the 0.4 cm tubes and, two of the 1.2 cm tubes were used, while only one of the large 2.2 cm tubes was used. A kinetic experiment started

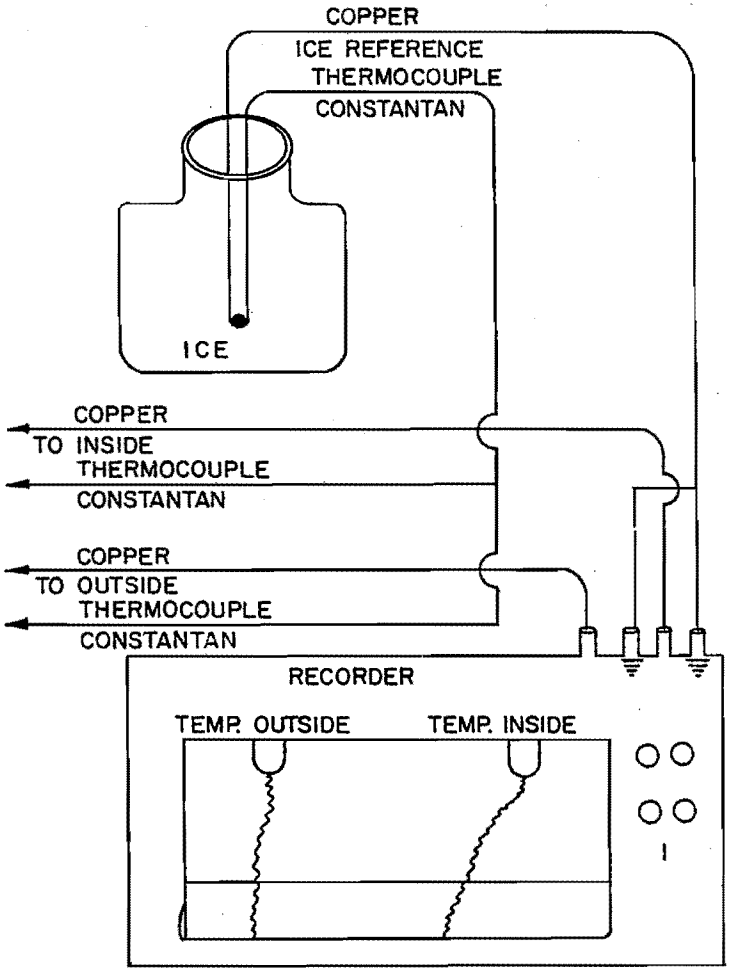

Figure 3. Two channel recorder wiring for thermal conductivity measurements.

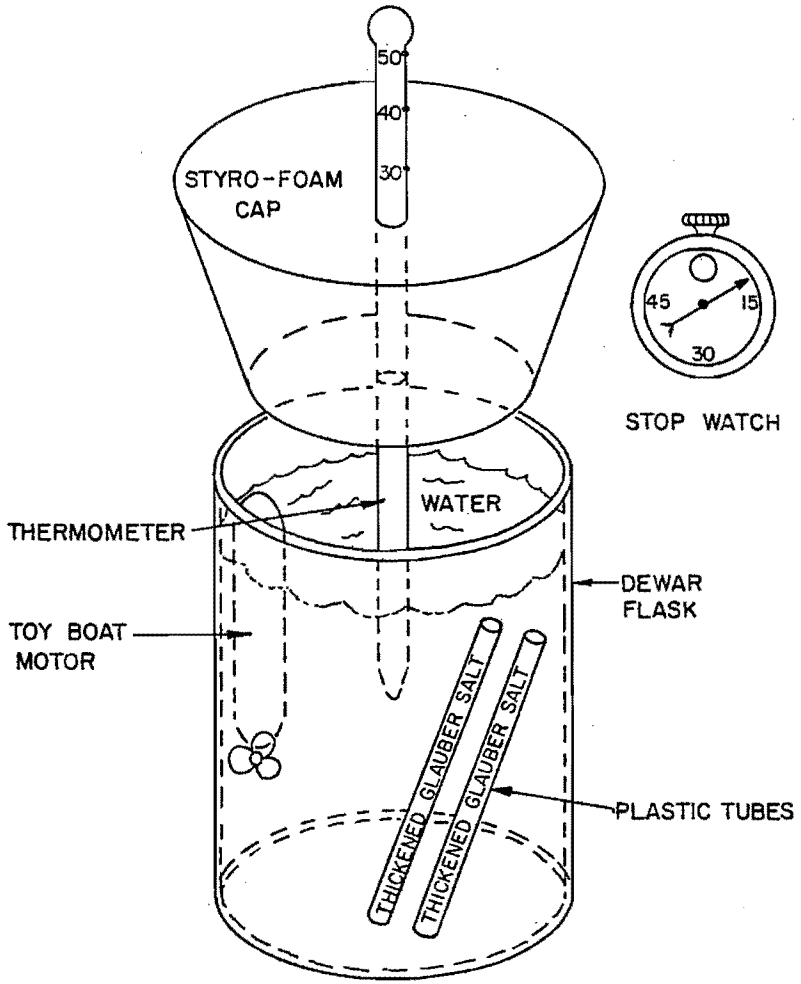

Figure 4. Stirred kinetic calorimetric apparatus.

with an appropriate number of tubes of material in a waterbath at a given temperature. The temperature of the waterbath and the ambient temperature were recorded. The temperature of the water in the Dewar flask was recorded just prior to dropping the tubes of material in, and a stopwatch was started as the tubes were dropped into the Dewar flask. The temperature was then recorded as a function of the elapsed time shown on the stopwatch for about 3 min at 5 sec intervals, with longer intervals as the heat transfer slowed. Rapid intervals were used at first with much wider intervals as the temperature change slowed.

Cycling Testing

In determining any degradation of material as a result of thermal cycling, it became necessary to construct a waterbath temperature cycler. The cycling chamber was a 2 liter Kimax™ aspirator bottle with bottom and top mounted side arms. Hot and cold water were alternately admitted to the bottom port and flow was continuous at about 3 to 4 liters/min for a 4 minute half cycle--then the water temperature at the bottom side arm inlet port was reversed for the next 4-minute half cycle. The temperature of the incoming hot water was about 60°C and the incoming cold water was around 15°C.

Water was delivered to the Kimax™ aspirator bottle from a washing machine solenoid valve. This 110 volt AC solenoid valve was activated alternately to the hot and cold water by a Double Pole Double Throw (DPDT) relay with activation coil potential of 24 volts DC. To prevent arcing of the 110 volt AC power across the relay contacts, two breaker contacts were wired in such a way as to produce a pair of series gaps in the inactivated circuit in both positions of the DPDT relay. The 24 volts necessary to activate the relay were supplied from a solid state binary counter chip amplified through a Darlington transistor amplifier circuit. An astable RC driven solid state chip supplied the primary frequency to the binary counter chip. The final cycle frequency could have been doubled several times or halved several times, but was never varied from the 8 minute total cycle time described earlier. (See Figure 5.) The 1.2 cm diameter tubes were cycled over 1500 times over a period of more than three months. Degradation was quantified during calorimetric kinetic studies by comparing observed to theoretical energy storage (Figure 5).

Aeration of Glaubers Salt

Concept

The fundamental difficulty involved in latent heat storage in incongruently melting materials such as Glauber salt is reversal of the decomposition reaction. In Glauber salt cycling this means the dissolution of anhydrous Na_2SO_4 and the subsequent recrystallization of this Na_2SO_4 as $Na_2SO_4 \cdot 10H_2O$. This process is seen as analogous to the oxidation of fuel in a furnace. If fresh oxygen-rich air is not brought into contact with the fuel, the reaction stops short of complete energy liberation. In the crystal furnace, water must be continually brought into contact with anhydrous Na_2SO_4 to allow dissolution and recrystallization as $Na_2SO_4 \cdot 10H_2O$.

The disadvantage of Herrick's rolling drum system and the problems encountered with the other reported systems prompted a search for a more effective method of agitating the salt solution. Sufficient agitation would prevent the anhydrous material from settling to the bottom and keep it dynamically interacting with free water molecules. The following five subsections briefly discuss experiments that were conducted which helped develop a better understanding of the problem and possible solutions.

Fluorescent Light Tube Reactor

Several burned out fluorescent light tubes were cut off at each end, cleaned, and fire polished. After cutting, these tubes were 65 ± 6 cm long by 36 mm inside diameter with a wall thickness of slightly under 1 mm. These tubes were fitted with #7 rubber stoppers with a single hole and a 6.4 mm glass tube. A fine mesh screen was used to support 2.5 cm of filter sand used to prevent anhydrous Na_2SO_4 from fouling the inlet tube at the bottom of the reactor. On all but one occasion, a cotton string was weighted with a glass stopper to provide a surface for crystal growth. A variable speed peristaltic pump was used to transport saturated solution back to the bottom port of the crystal reactor. The peristaltic pump was operating on a 1 cm outside diameter rubber surgical tube connected to both the top and bottom glass tubes placed in the #7 stoppers. These fluorescent tube reactors failed to settle the long thin crystals formed during rapid cooling. Plugging of the peristaltic pump and tubing was frequent and severe. Crystals even tended to form blocks in the fluorescent tube, which were then pumped to the top of the fluorescent tube blocking the outlet port.

Modified Separatory Funnel

In order to attempt to maintain high turbulence at the bottom of the reactor while allowing for anhydrous material to settle towards the bottom, a tapered reactor was conceived. A 1 liter pyrex separatory funnel was modified by having the valve removed and replaced by a simple 0.75 cm glass tube. This reactor chamber was then used in conjunction with a peristaltic pump. The reactor chamber was filled with recrystallized Glauber salt seeded with 3 g of borax ($Na_2B_4O_7 \cdot 10H_2O$) per 10 g of Glauber salt. Attempts with this solution recycle system proved fruitless due to crystallization in the tubing leading to and from the peristaltic pump (Figure 6).

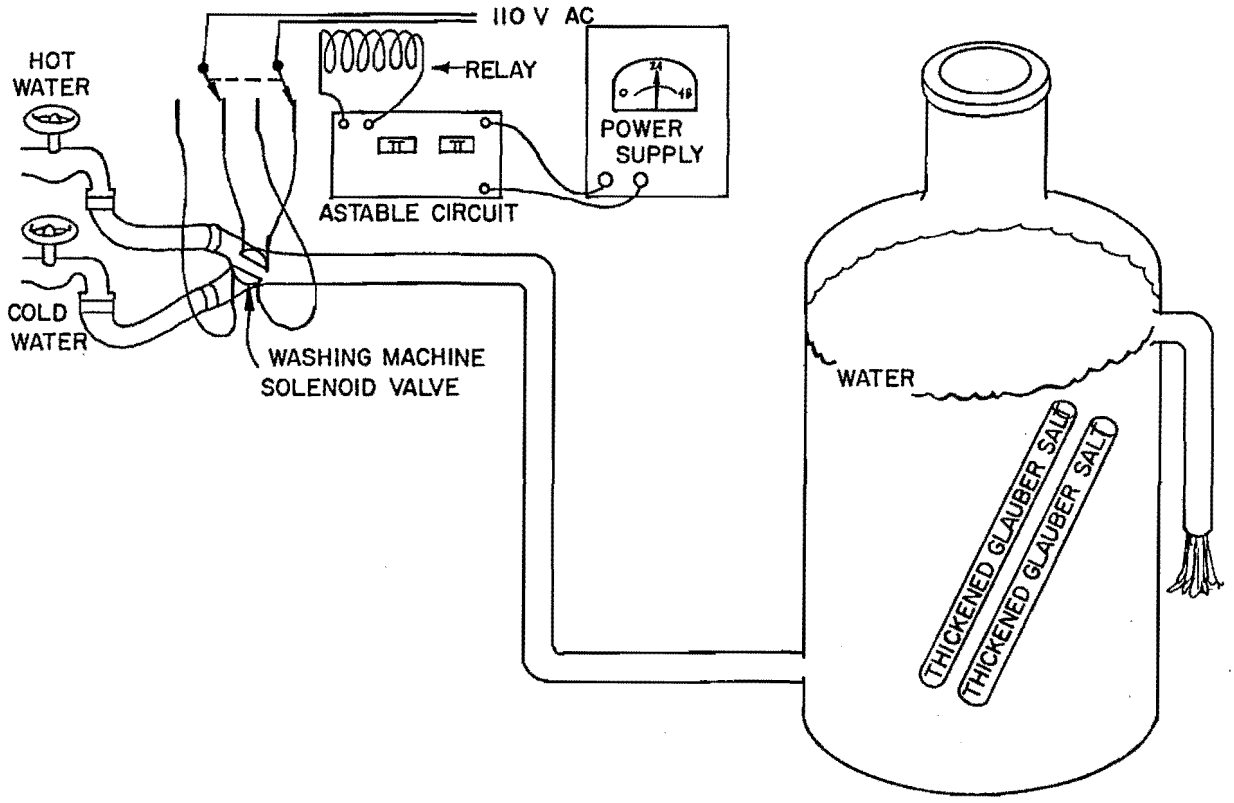

Figure 5. Cycle testing apparatus.

Heat Transfer from the Modified Separatory Funnel

A cooling experiment similar to that conducted on the Dewar flask was done on the modified separatory funnel. A small fan was used to supply air at about 3 m/sec to the outside of the separatory funnel. When filled with 1100 ml of water, the exponential cooling constant was 0.025/min giving a heat transfer coefficient of about 30 watts/m^2 °C.

Dye Concentration by Crystallization

The quantification of heat removal from any of these crystal reactor schemes proved to be difficult. It was observed, however, that recrystallization tended to concentrate impurities in the solution remaining after crystallization. After methylene blue was found to be insoluble in saturated Na_2SO_4 solutions, methyl-thymol blue was tried. Methyl-thymol blue proved to be extremely soluble. The higher pH of the saturated solution, above 8, maintained the pH sensitive methyl-thymol blue dye in its blue color state.

When a crystallization experiment was to be undertaken, a sample of Glauber salt from the stockpiles was recrystallized the day before the experiment. The day of the experiment the material was weighed on a scale and liquified by slow heating. At a temperature of about 38°C, when the incongruently melted mixture of anhydrous Na_2SO_4 and saturated solution contained no more large crystals of $Na_2SO_4 \cdot 10H_2O$, methyl-thymol blue dye was added to produce an optical density of approximately 0.15 at a wavelength of 610 nm. This optical density was determined on a spectrophotometer, with a 1 cm path length cuvette. The instrument was zeroed against distilled water. After addition of the dye, the material was vigorously stirred while 250 ml were siphoned off into a graduated cylinder. This material was magnetically stirred and cooled. At various time intervals, the optical density of the solution at a wavelength of 610 nm was determined. In addition, the amount of liquid that could be decanted out of the solids was quantified. At various times during the experiment, a balance was used to determine the weight of material solidified. A 250 ml graduated cylinder was used to quantify the volume of remaining liquid. The percent of $Na_2SO_4 \cdot 10H_2O$ crystallization as a function of optical density was determined from these data.

Air-stirred Crystal Furnace

The failure of attempts at recycling the saturated solution in the modified separatory funnel apparatus prompted the attempt at

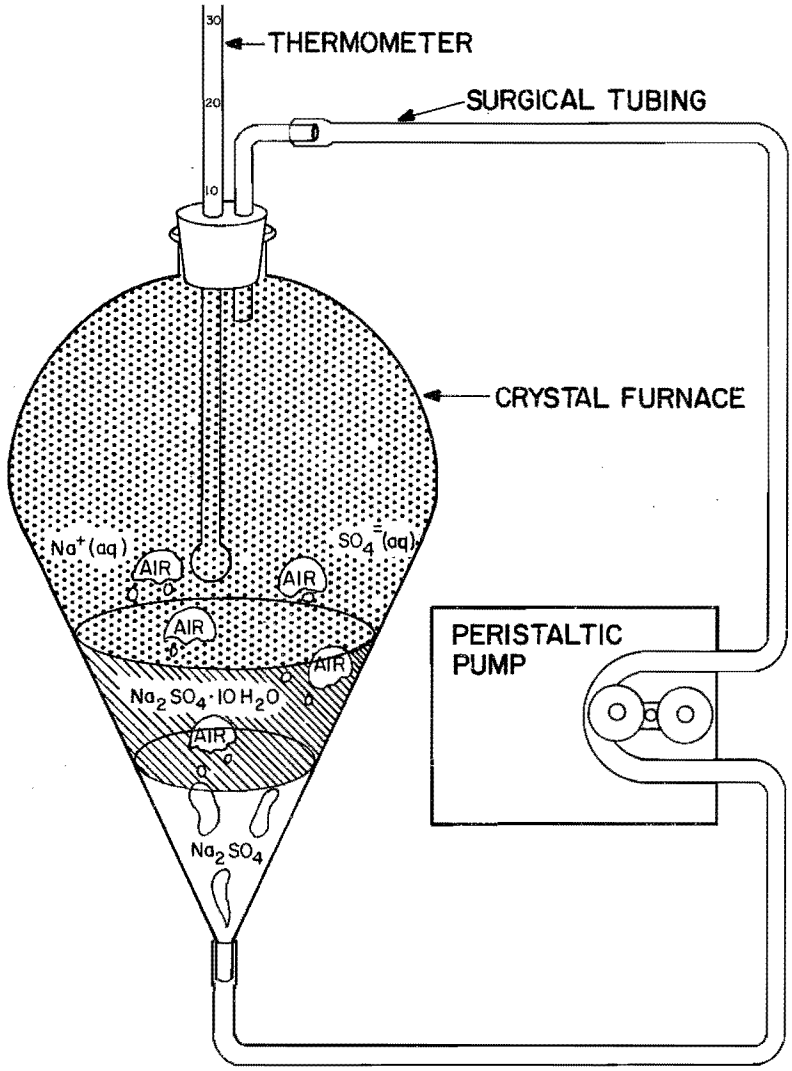

Figure 6. Stirred crystal furnace apparatus (in modified separatory funnel) (without air).

maintaining turbulence by bubbling air through the reactor. The air was initially supplied by a peristaltic pump equipped with surgical tubing (Figure 7). The only modification was the reduction of the volume in the modified separatory funnel, thus exposing the outlet port to the air space above the Glauber salt liquid. In the first operational experiment 800 g of methyl-thymol blue dyed and thermally "decomposed" Glauber salt was air stirred in the modified separatory funnel crystal furnace.

Favorable results of the aerated modified separatory funnel experiment prompted the construction of a larger aerated container illustrated in Figure 8. The unit is 110 cm long and 20 cm in diameter. It was filled with an 85 cm column height of Glauber salt crystals and fluidized with the addition of the 2 liters of water. Borax powder was used as a seeding agent and Cab-O-Sil thickness was added.

Due to the inefficient convective air heat transfer rates at the temperatures that will be normally encountered, a heat exchange pipe was placed inside the salt container. This 1 cm O.D. tube was used to heat the salt solution by running hot water, or for extracting heat by circulating cool water, through it.

Because of the increased column height of the salt in the larger test container, the peristaltic pump was found to have inadequate pressure to force air bubbles in at the bottom of the column. Consequently, a motor driven modified car tire pump was used. It

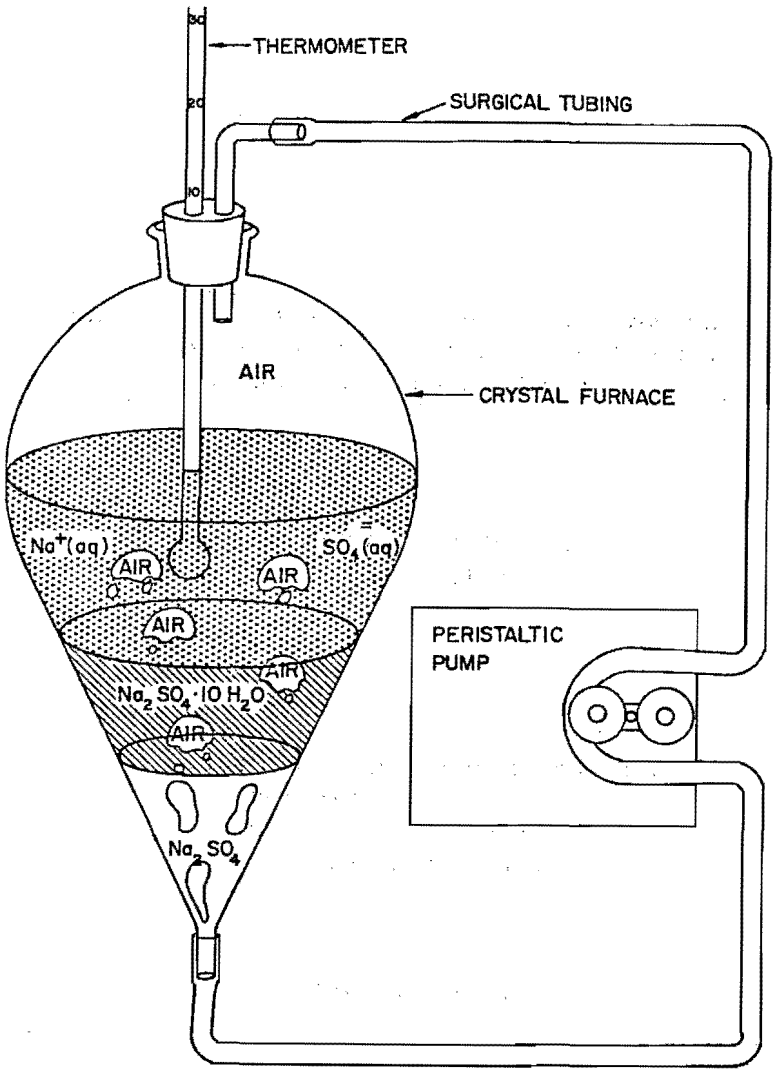

Figure 7. Stirred crystal furnace apparatus (in modified separatory funnel).

cycled once per second and displaced about 20 cc of air each strobe. Since the air was withdrawn from the top of the column and reintroduced at the bottom of the column, no moist air escaped into the atmosphere which would otherwise tend to gradually dehydrate the salt solution. To prevent salt from crystallizing in the air tube a check valve was placed at the air discharge point. It was made from a 7 cm x 1 cm diameter length of surgical tubing plugged on one end and stretched over the tip of the air supply tube. A small slit was cut in the tube with a razor blade. Air would expand the slit sufficiently to escape on the pressure cycle, then the tube would close during the air intake part of the cycle.

To further alleviate salt plugging problems in the air line in the event the check valve leaked, a 20 gage nichrome teflon-covered resistance wire loop was inserted the full length of the air supply line. Whenever plugging did occur, due to periods of non use, it could be cleared by running electric current through the resistance wire. This heat would melt the salt crystals, and the applied air pressure would gradually purge the fouled air line and normal operation could be resumed.

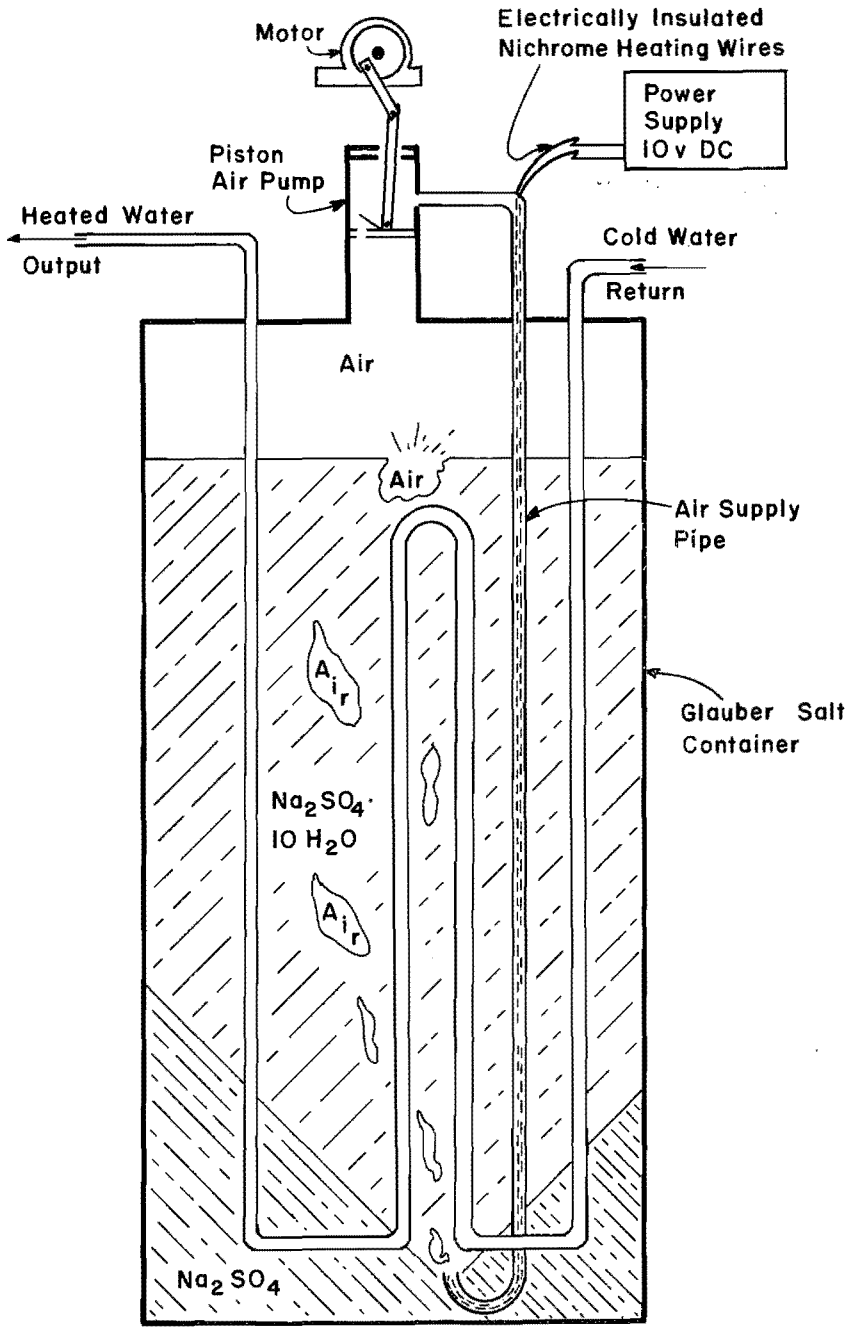

Figure 8. Aerated Glauber salt furnace with water pipe heat exchanger.

RESULTS AND DISCUSSION

Thermal Conductivity

Knowledge of coefficients for thermal conductivity of heat storage material is important in order to design for adequate heat exchange. Consequently, a thermal conduction test set-up was designed and several tests were run on Parowax, whose thermal conductivity was already known. Tests were also conducted on various formulas of Glauber salt and thickener whose thermal conductivities were not known.

Amoco Parowax

The relationship of thermal conductivity to the interior or maximum temperature is shown in Figure 9. The thermal conductivity decreases from a value of about 0.41 watts/m°C at 25°C to a value of about 0.32 watts/m°C at 50°C. The melting temperature of this wax is about 50°C and the increasing conductivity observed above 50°C is at least partially, if not totally, due to free convective heat transfer across an increasing liquid annulus around the heated interior copper tube. These values are about twice as high as those reported in the International Critical Tables (Washburn 1929) for paraffin wax.

These data were all obtained with the shortest length concentric tube apparatus on the two channel recorder. These data indicate that any drift in the two channel recorder is most probably not sufficient to account for more than about $\pm$ 0.02 watts/m°C of thermal conductance.

Glauber Salt Solid

The thermal conductivity of pure recrystallized Glauber salt is related to the maximum or interior temperature as shown in Figure 10. The thermal conductivity of the material around 80°C is about 0.60 $\pm$ 0.008 watts/m°C. With all the data included, the thermal conductivity of this sample of Glauber salt seems to be 0.60 $\pm$ 0.08 watts/m°C. Based on these data, no variational trend of thermal conductivity with temperature was observed.

The melting temperature was never exceeded for fear that separation of anhydrous sodium sulfate from the saturated solution would generate irreversibly inhomogeneous layering in the thermal conductivity apparatus. The values were again high, but were within 50 percent of the thermal conductivity of 0.51 watts/m°C reported for Glauber salt in the literature (Jurinak and Abdel-Khalik 1978).

Cab-O-Sil Thickened Glauber Salt

The thermal conductivity of thickened suspensions of Glauber salt was found to vary extensively regardless of the combinations of equipment used. No trend in thermal conductivity could be discovered in the data (Figure 11). The mean thermal conductivity was 0.61 $\pm$ 0.18 watts/m^2 °C. These data have a coefficient of variation of over 30 percent. A further discussion of these data is presented in Appendix A.

Astro Gum 21 Starch Gel

Numerous attempts were made to thicken borax seeded Glauber salt with the modified corn starch. This carboxy-methyl-amylose material comes in several different grades; Astro Gum 3010 and Astro Gum 21 were tested.

While neither of these gel materials could be kept in suspension at the high ionic strength of saturated sodium sulfate solutions, thermal conductivity tests were run on an Astro Gum 21 gel.

The data are not sufficient to warrant a trend analysis. As illustrated in Figure 12, the thermal conductivity does seem to decrease with increasing temperature. While the gel was extremely thin and somewhat inhomogeneous with thicker firmer lumps included, the decreasing thermal conductivity would not be expected if convective heat transfer was interfering.

The higher values of thermal conductivity (over twice that of Cab-O-Sil thickened Glauber salt) show promise of improving the heat transfer in thickened Glauber salt suspensions. The insolubility of starches in saturated solutions of sodium sulfate extends to soluble potato starch. The disaccharide maltose, however, will remain soluble in saturated sodium sulfate solution. If the thermal conductivity of starch gels is ever to be advantageous in Glauber salt thickening, more soluble starches must be used. This confounds the thickening properties by leading to more easily thinned gels, since

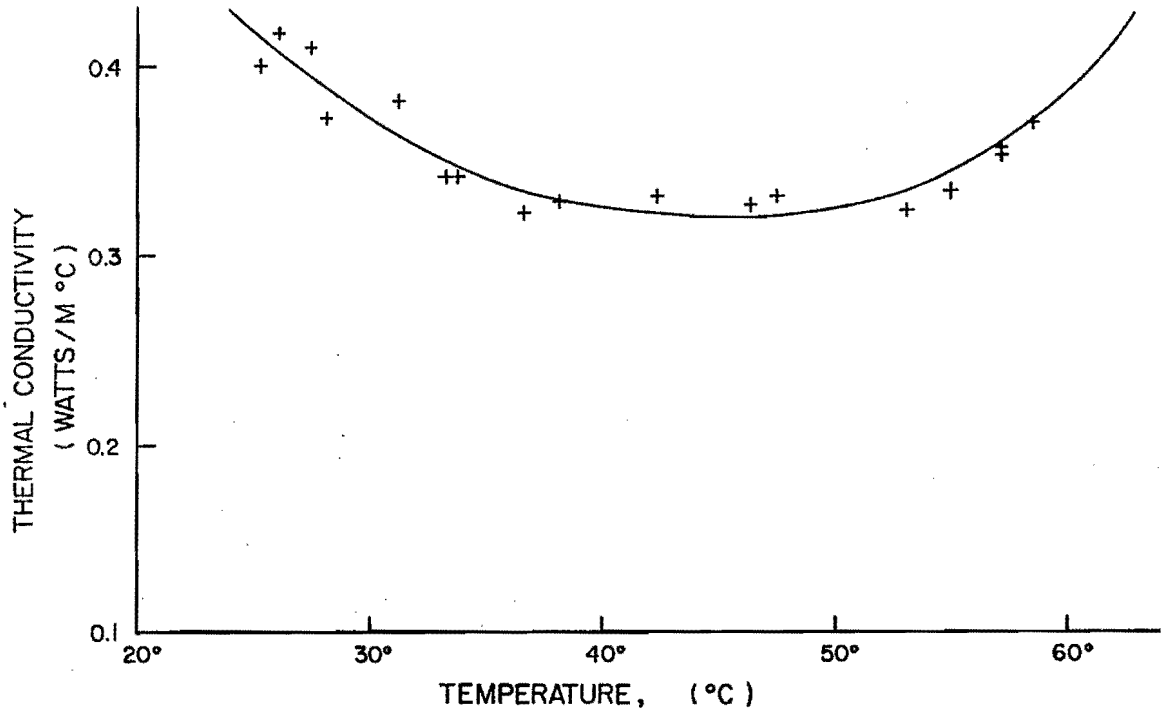

Figure 9. The thermal conductivity of Amoco Parowax (determined experimentally).

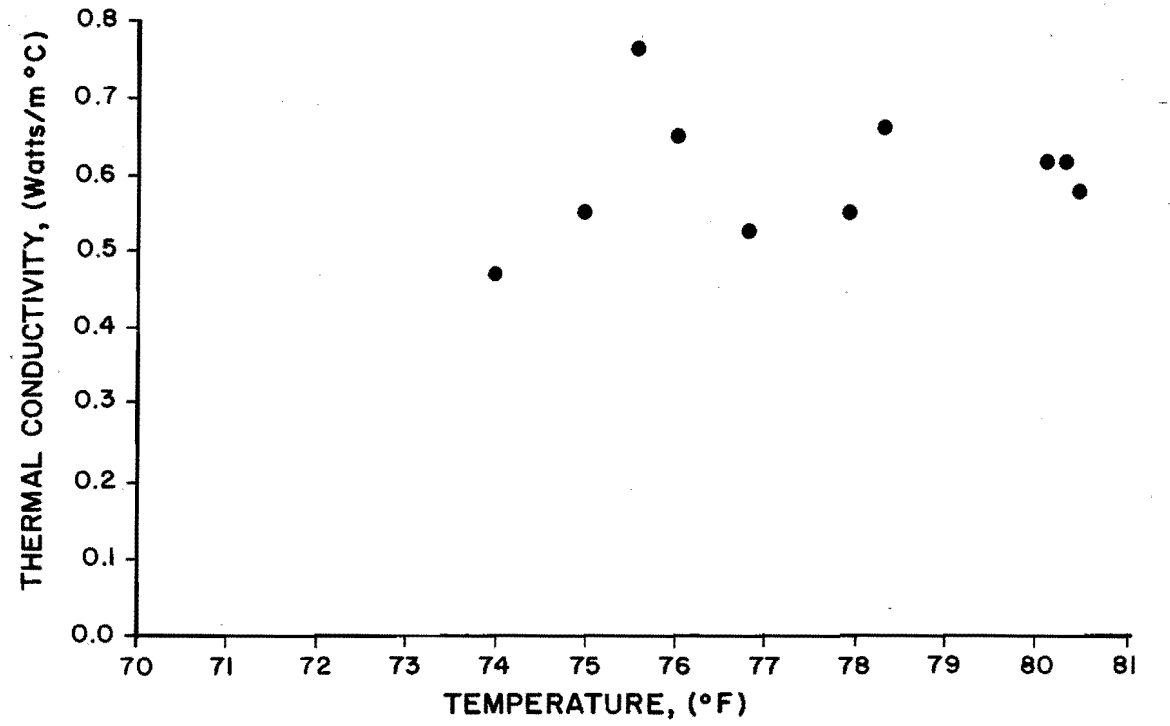

Figure 10. The thermal conductivity of unmodified Glauber salt (experimental results).

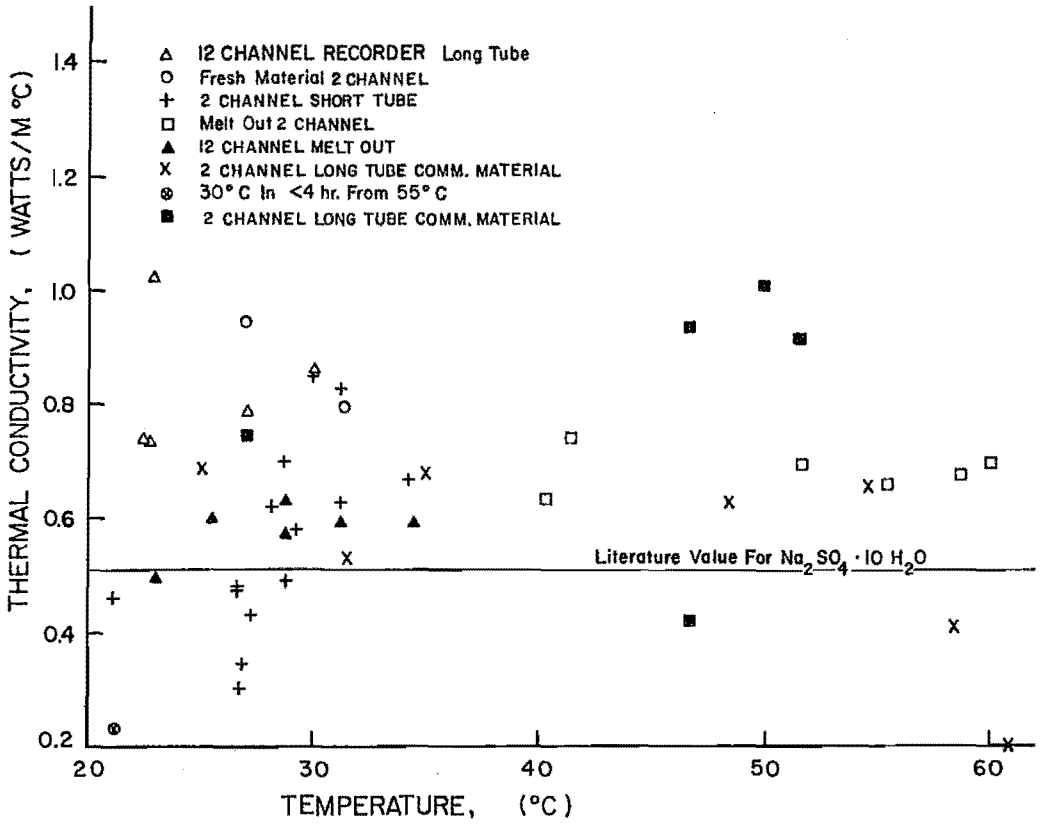

Figure 11. The thermal conductivity of Cab-O-Sil gelled $Na_2SO_4 \cdot 10H_2O$.

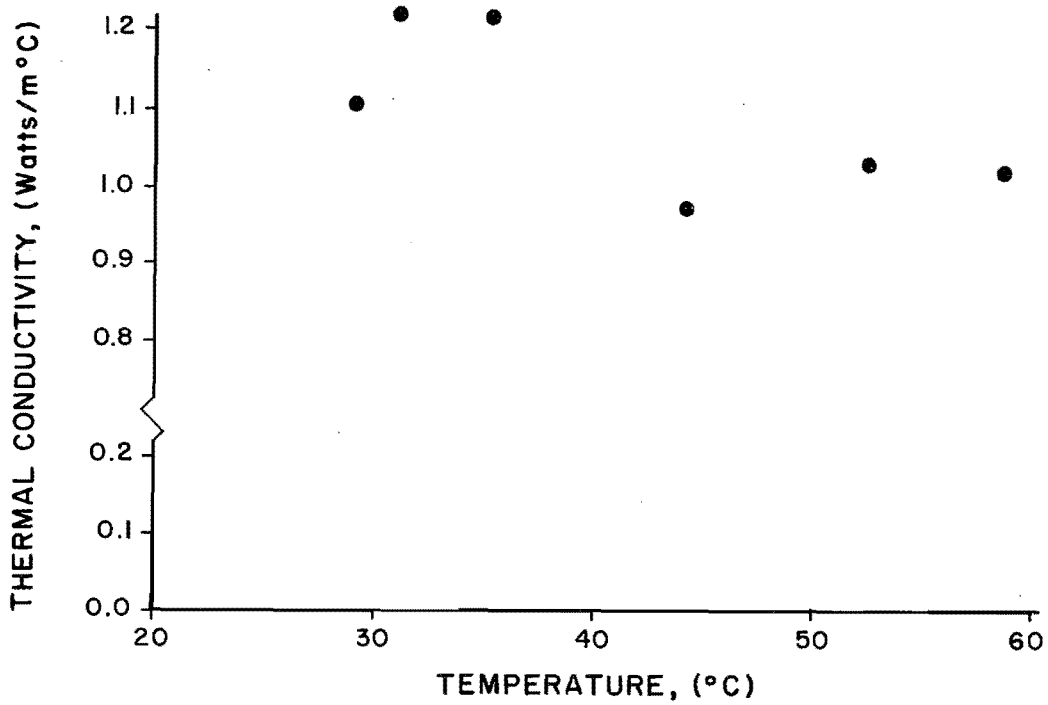

Figure 12. Thermal conductivity of a thin Astro Gum 21 gel.

the thixotropic nature of the gel is only needed when the ten waters of hydration are released. Dilution of the gel occurs when thickening is desired.

Mathematical Modeling

The differential equation governing transient heat conduction is:

$$\partial^2 T/\partial x^2 + \dot{q}/k = \rho c/k \; \partial T/\partial \tau \quad . \; . \; . \; . \; . \; . \quad (11)$$

where

$\partial^2 T/\partial x^2$ = second partial of temperature in the space dimension normal to heat transfer (T/L^2)

$\dot{q}$ = heat transferred per unit time per unit volume ($E/L^3 t$)

k = thermal conductivity of the material conducting the heat (E/LTt)

ρ = density of the material (M/L^3)

$\partial T/\partial \tau$ = first partial of the temperature change with time (T/t)

for one dimensional heat transfer through a flat sheet of material. If we change to radial heat flow, the differential equation in cylindrical coordinates is:

$$\partial^2 T/\partial r^2 + 1/r \; \partial T/\partial r + \dot{q}/k = \rho c/k \; \partial T/\partial \tau \quad . \; . \; . \quad (12)$$

where the variables are the same as above. It can be seen that by allowing radial heat transfer, the rate of change of temperature with time is increased by the term $1/r \; \partial T/\partial r$. For spherical coordinates with uniform radial flow, the heat transfer is even greater:

$$1/r \; \partial^2 (rT)/r^2 + \dot{q}/k = \rho c/k \; \partial T/\partial \tau \quad . \; . \; . \quad (13)$$

where the variables are again defined as above.

Cylindrical heat flow will be considered for the remainder of the discussion. This is done because the manufacture of spherical containers is anticipated to be several fold more expensive than the simple manufacture of tubes.

The simplest case and the most desirable from a heat availability standpoint is a larger external resistance to heat transfer in comparison to the internal resistance to heat transfer. These are the conditions of lumped heat flow analysis. The problem becomes the simultaneous solution of the internal energy change equation and the convective heat loss equation.

$$c\rho V \; dT/d\tau = q = hA(T_{wall} - T_{bulk}) \quad . \; . \; . \quad (14)$$

where

c = specific heat of the material (E/MT)

ρ = density of the material (M/L^3)

dT/d = rate of change of temperature

q = rate of heat transfer (E/t)

h = convective heat transfer coefficient (E/L^2Tt)

A = surface area of the body (L^2)

$T_{wall}-T_{bulk}$ = temperature difference between the wall of the body and the bulk of the surrounding fluid (T)

The solution to these equations is:

$$\frac{T_{wall}(\tau) - T_{bulk}}{T_{wall}(0) - T_{bulk}} = \exp\,(-(hA/c\rho V)\tau) \quad . \; . \; . \; . \quad (15)$$

where

$T_{wall}(\tau)$ = temperature of the wall at time τ(T)

$T_{wall}(0)$ = initial temperature of the wall of the container (T)

With latent heat, the internal energy is not only in the form of sensible heat capacity, but is also in the form of chemical potential energy. Before the heat can be transported through the material, however, it must be liberated as thermal energy. Thus, if a substitute heat capacity of the Glauber salt package under consideration can be defined as:

$$c' = (H + c\Delta T)/\Delta T \quad . \; . \; . \; . \; . \; . \; . \quad (16)$$

this theory of cooling can still be used. In the above equations:

V = volume of body (L^3)

H = latent heat of fusion per unit mass (E/M)

ΔT = rate of change of temperature (T)

Holman (1972) reports that this approximation of "lumped heat" is valid when:

$$(h/k)(V/A) < 0.1 \quad . \; . \; . \; . \; . \; . \; . \quad (17)$$

where the other variables are as defined above with k being the thermal conductivity of the "lumped mass." For cylinders the volume to surface area ratio is the diameter divided by four. Thus, tubes of material should cool approximately exponentially when:

$$h < 0.4k/d \quad . \; . \; . \; . \; . \; . \; . \; . \quad (18)$$

where d is the diameter of the cylinder and h and k are defined above. For Glauber salt tubes of thermal conductivity of approximately 0.61 watts/m°C, a diameter of 1 cm requires a convective heat loss coefficient

less than 24.4 watts/m^2 °C. Free convective heat transfer from tubes of such size is about 7.6 watts/m^2 °C leaving some room for forced convection. For larger, cheaper-to-package 2 cm diameter tubes, the maximum tolerable convective transfer is only 12.2 watts/m^2 °C. Free convective transfer from horizontal tubes of such dimensions is approximately 6.4 watts/m^2 °C. The tubes should be placed horizontally to minimize separation of the Glauber salt. For very small tubes, say 0.5 cm in diameter, the convective heat loss needs to be less than 48.8 watts/m^2 °C. Free convective losses for this size tube (approximately 10 watts/m^2 °C) could be moderately increased by forced convection and still not exceed the limits of total heat availability at the outside surface of the cylinder.

The heat generated from rest mass conversion (i.e., chemical potential) aids in maintaining a constant exterior surface temperature. This makes the design by "lumped capacity" quite conservative.

Thin Film Polyethylene Packaging

Exponential Cooling

In light of the high convective heat transports observed in water and Equation 13, "lumped heat" analysis might seem futile on any moderately sized tube of Glauber salt. Preliminary results indicated that 1 cm diameter tubes could serve as fairly constant temperature heat sources. Figures 13, 14, and 15 are representative of a wealth of kinetic calorimetric data collected on 2.2 cm, 1.2 cm, and 0.4 cm diameter polyethylene tubes dropped into a Dewar flask water bath. No coefficient of determination (R-SQ) for these log-linear fits was ever observed to be below 0.92 and for water temperatures more than 5°C from the melting temperature, coefficients of determination never dipped below 0.99.

The lumped analysis of heat flow is in fact possible for a two temperature system such as tubes of Glauber salt in water, by solution of a pair of differential equations like Equation 9 simultaneously (see Figure 4)

$$c'_{Gl}\rho_{Gl}V_{Gl}dT_{Gl}/d\tau = hA(T_{wa} - T_{Gl}) \quad . \quad . \quad . \quad (19)$$

$$c_{wa}\rho_{wa}V_{wa}dT_{wa}/d\tau = hA(T_{Gl} - T_{wa}) \quad . \quad . \quad . \quad (20)$$

where

c'_{Gl} = apparent specific heat of Glauber salt (including latent heat (E/MT)

c_{wa} = apparent specific of water (E/MT)

ρ_{Gl} = density of Glauber salt (M/L3)

ρ_{wa} = density of water (M/L3)

V_{Gl} = volume of Glauber salt (L^3)

V_{wa} = volume of water (L^3)

T_{Gl} = temperature of Glauber salt (T)

T_{wa} = temperature of water (T)

τ = elapsed time after thermal contact (t)

h = convective heat transfer coefficient (E/L^2Tt)

A = surface area exposed to convectin (L^2)

The solution is again exponential.

$$\frac{(T_{wa}(\tau) - T_{eq})}{(T_{wa}(0) - T_{eq})} = \exp(-hA(1/c'_{Gl}\rho_{Gl}V_{Gl} + 1/c_{wa}\rho_{wa}V_{wa})\tau) \quad . \quad . \quad . \quad . \quad . \quad . \quad . \quad . \quad (21)$$

The complimentary equation for the Glauber salt is:

$$\frac{(T_{Gl}(\tau) - T_{eq})}{(T_{Gl}(0) - T_{eq})} = \exp(-hA(1/c'_{Gl}\rho_{Gl}V_{Gl} + 1/c_{wa}\rho_{wa}V_{wa})\tau) \quad . \quad . \quad . \quad . \quad . \quad . \quad . \quad . \quad (22)$$

where c'_{Gl} is as defined by Equation 16 and the other variables are as defined above. It might be expected that the sensible heat on both sides of the melting point would produce a different temperature response than the chemical kinetic response of latent heat. Figure 14 indicates that the first five or six points do indeed have a greater slope than the remaining points, and the last two or three points have a slightly larger slope than the central points do, also. Figure 15 is the same data with the first five and last three points eliminated. A high or a low initial slope can occur as a result of a high or low estimate of the equilibrium or final temperature, respectively.

Regardless of the reasons for the deviations when the external temperature is near the melting temperature, at temperatures more than approximately 10°C from the melting temperature, even 2.2 cm tubes release heat in almost perfect exponential fashion. The values of the exponential cooling constants as a function of initial external temperature are found graphically presented in Figure 16.

It is apparent from Figure 16 that freezing is a slightly slower process than melting, for equal temperature difference from the melting point. By using the relationship:

$$h = \text{slope}/A\ (1/c_{wa}\rho_{wa}V_{wa} + 1/c'_{Gl}\rho_{Gl}V_{Gl}) \quad . \quad . \quad . \quad (23)$$

where

h = average heat transfer coefficient (E/L^2Tt)

slope = found from a cooling history plotted exponentially against time

A = surface area (L^2)

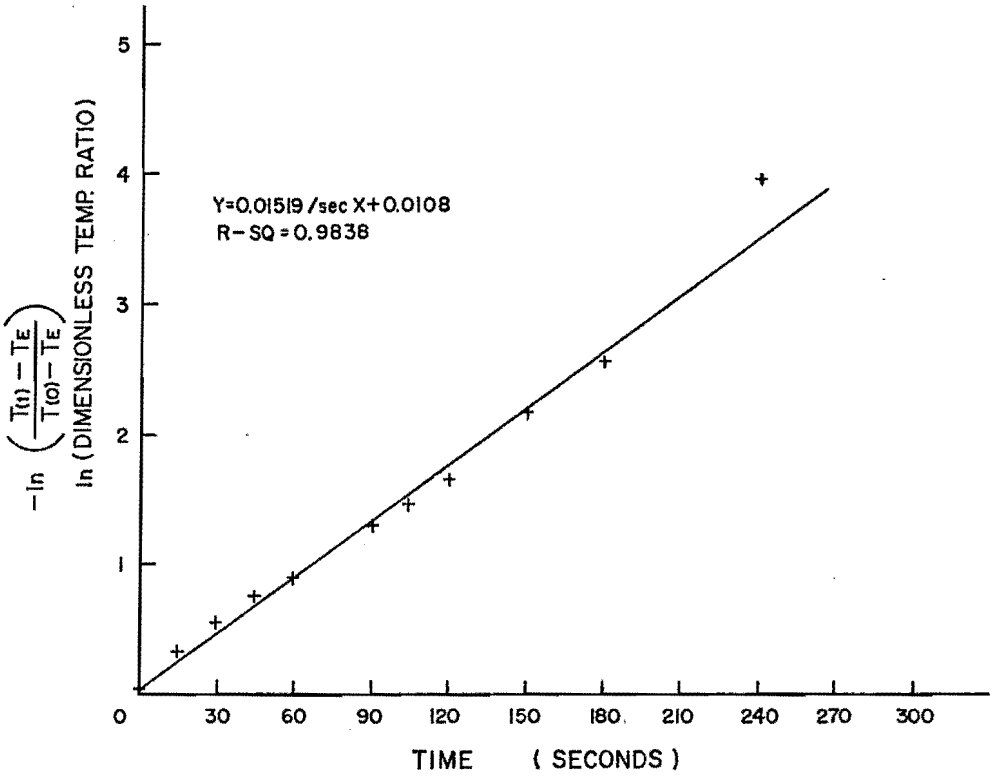

Figure 13. Decomposition heat uptake by two 1.2 cm diameter packets of solar salts in 500 ml of tap H_2O.

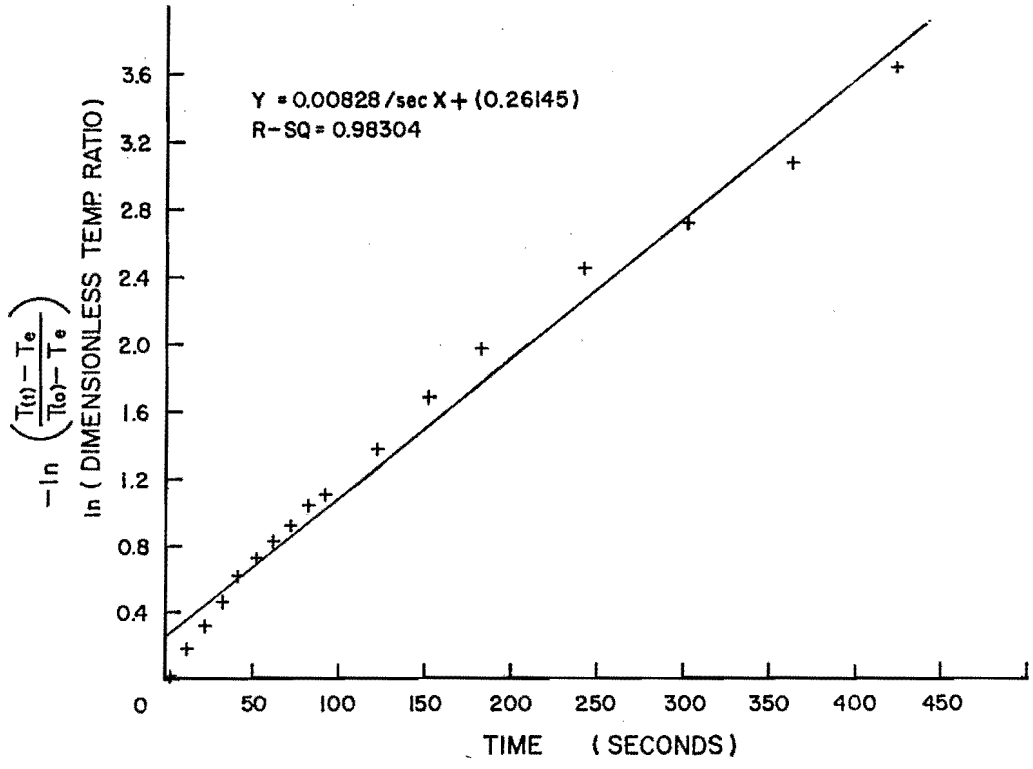

Figure 14. Crystallization heat release by two 1.2 cm diameter packets of solar salts in 500 ml of tap H_2O.

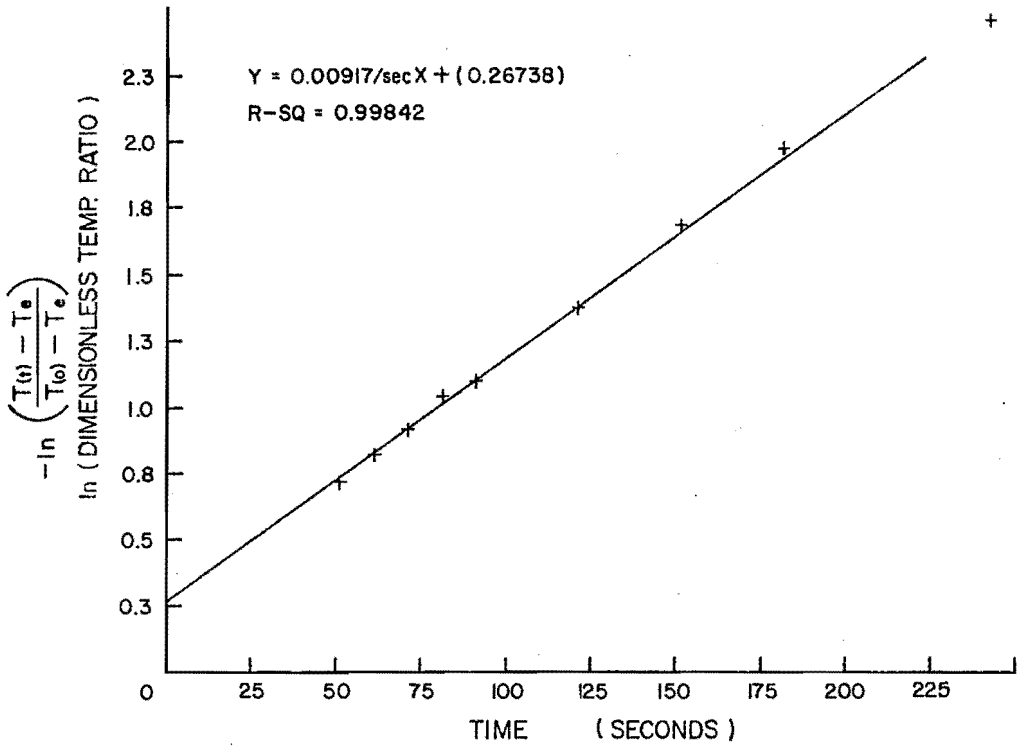

Figure 15. Crystallization heat release by two 1.2 cm diameter packets of solar salts in 750 ml of tap H_2O.

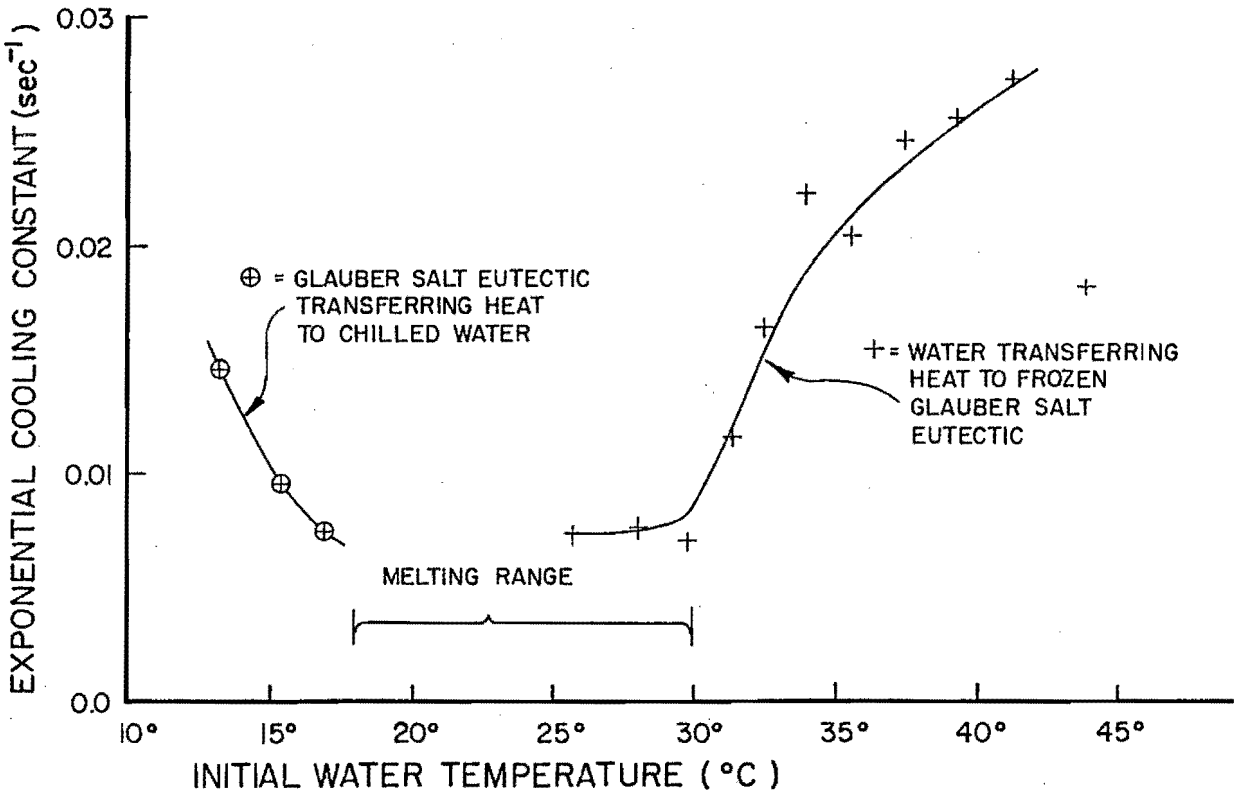

Figure 16. Exponential cooling constants as a function of initial water temperature.

c_{wa} = apparent heat capacity for water (E/MT)

c_{Gl} = apparent heat capacity for Glauber salt (E/MT)

V_{wa} = volume of water in the Dewar flask (L^3)

V_{Gl} = volume of Glauber salt in the Dewar flask (L^3)

ρ_{wa} = density of the water (M/L^3)

ρ_{Gl} = density of the Glauber salt (M/L^3)

an estimate of the film convection constant h can be obtained.

A more in-depth analysis would involve a study of the transient temperature history of the interior of the freezing tube of material. Carslaw and Jaeger (1959) have shown that the equation:

$$2R^2 \ln(R/a) - R^2 + a^2 = (4k_s(T_{melt} - T_{ext})/H\rho)\tau \quad . \quad . \quad . \quad . \quad . \quad . \quad . \quad . \quad (24)$$

where

R = radius of remaining liquid core (L)

a = radius of the tabular containment (L)

k_s = thermal conductivity of the solidified outside annulus (E/LTt)

$T_{melt}-T_{ext}$ = temperature difference between the melting point and the exterior of the containment (T)

$H\rho$ = latent heat energy density found by multiplying the latent heat times the density of the latent heat material (E/L^2Tt)

τ = time since initiation of freezing (t)

is a good approximation to the time dependence of the location of the freezing interface in a cylindrically freezing system with constant temperature maintained at radius a. The situation and differential equation are outlined in Figure 1. The latent heat liberated (Q) when the interface is at R is:

$$[(a^2 - R^2)/a^2](H\rho V) = Q \quad . \quad . \quad . \quad . \quad . \quad . \quad . \quad (25)$$

where the variables are as defined above. This permits linear arrangement of this cooling function. The resulting linear form is:

$$F[T(\tau)] = [T(\tau)-T(0)] + 2[T_{eq}-T(0)]\left[\left(1-\frac{[T(\tau)-T(0)]}{[T_{eq}-T(0)]}\right)\cdot\left(\ln\sqrt{1-\frac{[T(\tau)-T(0)]}{[T_{eq}-T(0)]}}\right)\right] = \left(\frac{(T_{melt}-T_{eq})[T_{eq}-T(0)]4k_s}{H\rho a^2}\right)\tau \quad . \quad . \quad . \quad (26)$$

where

T_{eq} = final equilibrium temperature after heat exchange (T)

$T(\tau)$ = temperature of the water bath as a function of time $\tau(T)$

$T(0)$ = initial temperature of the water in the bath (T)

Other variables are as defined above.

Coefficients of determination are all above 0.81 (R-SQ), but were generally smaller than those for simple exponential cooling or warming. The data consistently show a concave increase in slope. There are a number of idealizations in this theory that are violated by the material under study (see Figures 17 and 18). The principle non-ideality is the supercooling observed with Glauber salt. This phenomenon causes an ever widening annulus of crystallization, or freezing interface. This may be the cause of the nonlinearity of the transformed data.

The advantage of this theory is its prediction of a finite cooling time. Taking the limit as R approaches 0 to determine the time to complete freezing (τ_{max}) gives:

$$\tau_{max} = a^2H\rho/(T_{melt} - T_{eq})4k_s \quad . \quad . \quad . \quad . \quad (27)$$

where the variables are defined as those in Equation 24. This is the relationship of the freezing time to the radius of the frozen tube. This theory fits well within the accuracy of measurements of H and k_s. The observed average cooling rate for crystallization of the three sizes of tubes studied is presented in Figure 19.

Degradation

The hampered reversibility of the incongruent melting or decomposition reaction was studied by cycling the material in approximately 50°C water alternated with about 15°C water. The "degradation" was both observed in the form of small hard white chunks, resembling anhydrous sodium sulfate in appearance, and quantified as the percentage of the theoretically available heat that was never realized. With the commer-

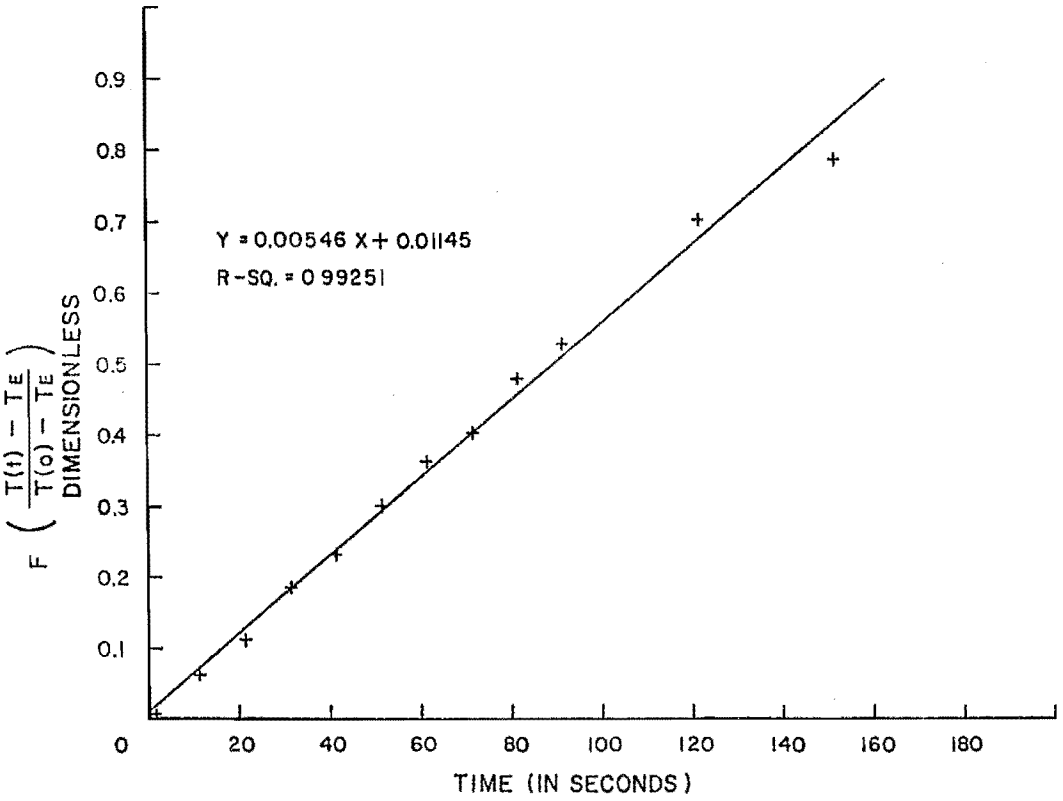

Figure 17. Crystallization heat release by two 1.2 cm diameter packets of solar salts in 750 ml of tap H_2O.

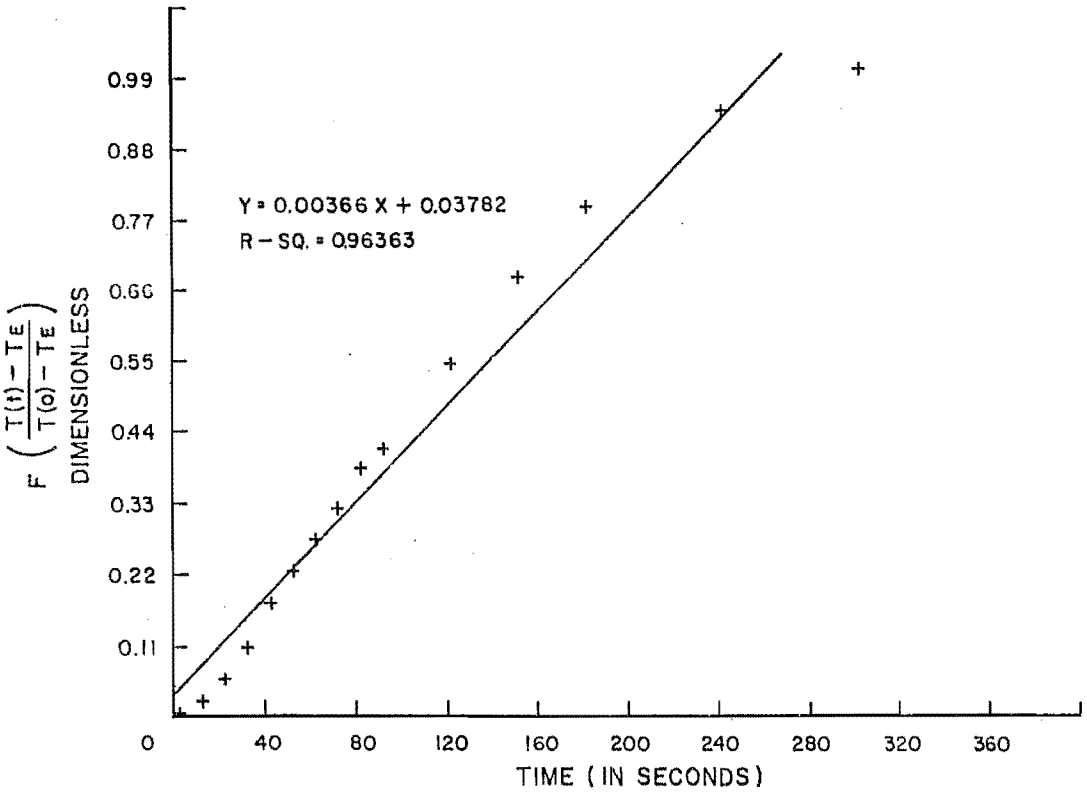

Figure 18. Decomposition heat uptake by two 1.2 cm diameter packets of solar salts in 500 ml of tap H_2O.

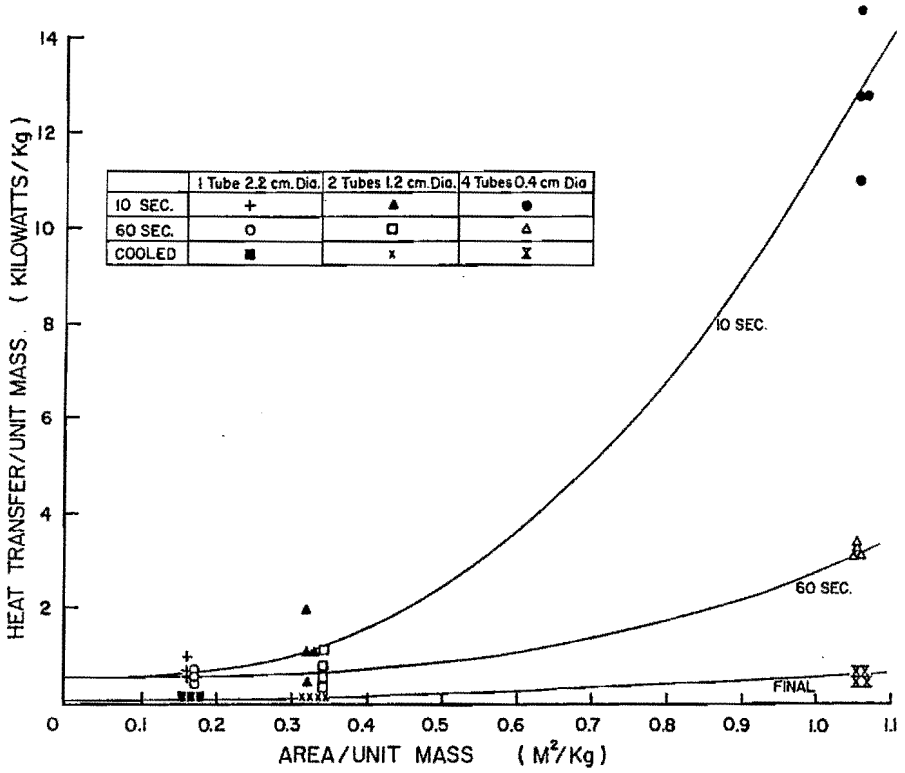

Figure 19. Average heat rates of three sizes of tubes of thickened Glauber salt.

cially prepared solar salts, degradations were on the order of 40 to 60 percent. No relationships could be found between number of cycles and degradation.

Available energy seemed to be predominantly a function of crystallization time. This would be expected since all the theoretically available energy should ultimately be extractable from salt of any age or history. The degradation is kinetically controlled; the time for diffusion to act on larger lumps of anhydrous sodium sulfate is greater than the time required to diffuse from smaller particles. Larger lumps were observed in the bottom of tubes held vertically than those held horizontally, indicating settling and accumulation of the irreversible material.

The possibility exists that a slight addition of extra water and thickener above that stoichiometrically required would help to continuously cycle more of the material.

Crystallization Furnace

Recycling of Fluid

The pumping of saturated solution from the top of the modified separatory funnel crystallizer invariably lead to plugging. Plugging occurred in the tubes leading to or from the pump or in the peristaltic pump itself. Rapidly grown crystals were observed to be extremely long and thin on the order of 10 to 20 times longer than wide. This is in direct contrast to the large angular nearly cubic nuggets which crystallize out in slowly cooled containers. These long thin crystals lead to extremely slow settling velocities and a considerable crystal carry over through the external tubing and pump. There is a good possibility that if the pump inlet tube, the pump, and the return flow tube were heated sufficiently, pump plugging by crystallization would not occur; nor would this applied heat be lost since it adds to the overall heat stored in the salt.

When air is pumped through the separatory funnel reactor, the plugging which occurs can be worked back out of the rubber tubing. The calibration of the methyl-thymol blue response to crystallization concentration is shown in Figures 20 and 21. The calibration was done as described in the materials and methods section on a separate flask magnetically stirred. The data are roughly hyperbolic and the exclusion of dye into the remaining fluid with increasing crystallization should generate hyperbolic concentration. Thus the regression was done on the hyperbolic transformation of the data. This hyperbolic transformation of the axis is used in Figure 21.

The release of latent heat is estimated for the modified separatory funnel crystal-

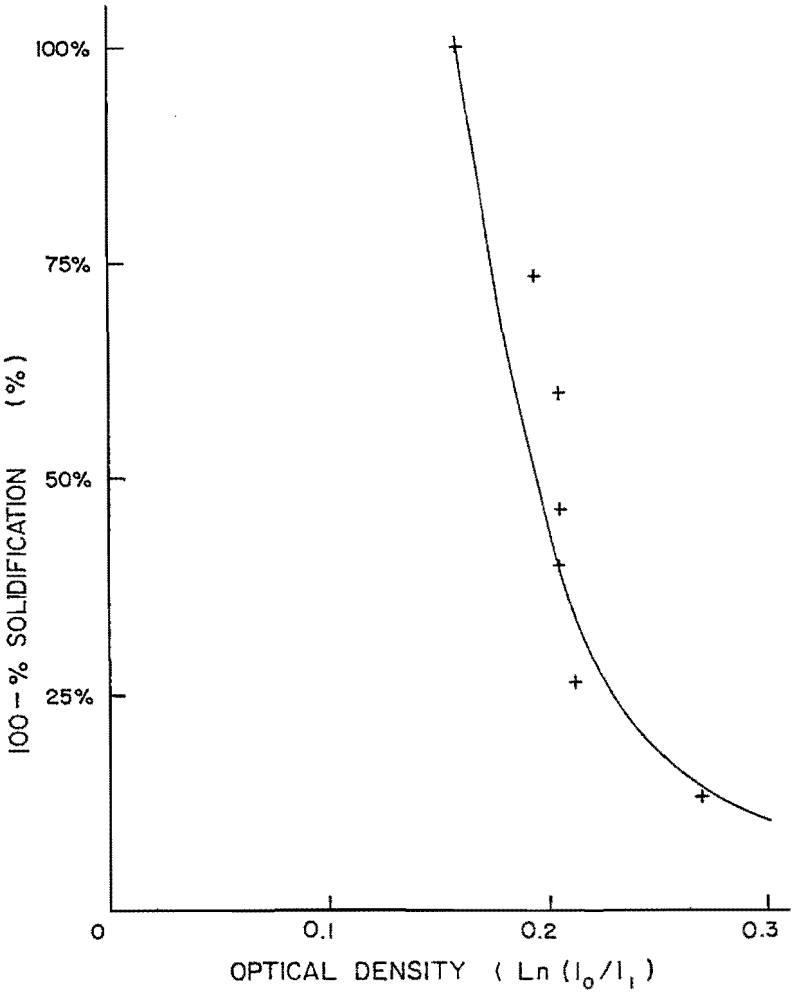

Figure 20. Calibration curve for solidification concentration of methyl-thymol blue.

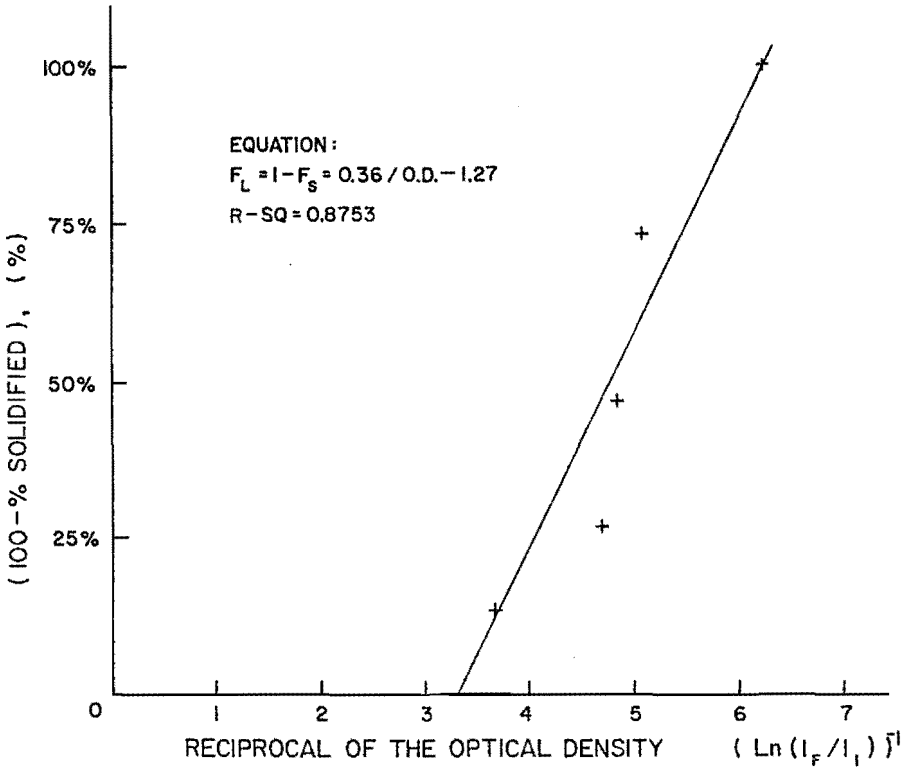

Figure 21. Regression of calibration for methyl-blue concentration upon crystallation.

lization reactor with an external air velocity at the periphery of 3.6 m/sec. The rate of crystallization is shown in Figure 22. No obvious nonlinearity was observed so it is assumed that crystallization proceeded at a constant rate from 0 percent Glauber salt crystallization to 94 percent Glauber salt crystallization. Unfortunately, nearly 100 g or 14 percent of the material was spilled and lost during the experiment, but it is felt that the estimated heat release of 0.38 kW/m^2 was moderately accurate.

Enlarged Air Stirred Furnace

The enlarged air-stirred furnace held 23 liters of salt crystals and 2 liters of water. Since the theoretical heat of fusion for Glaubers salt is 60.5 cal/gm, and its density is 1.46, it has an energy storage capability of 89 cal/cm^3 (10,000 Btu/ft^3) (Telkes 1980). The theoretical fusion energy stored in the test furnace is therefore

$$23{,}000\ cm^3 \times 89\ cal/cm^3 = 2.05 \times 10^6\ cal = 8{,}567\ kj$$

In addition if the temperature changes from 34.4 to 24.1°C there is an additional energy release of approximately 1100 kJ. If the specific heat of the salt solution and salt crystals are added to the heat of fusion, the combined energy stored is approximately 9700 kJ. During tests conducted on the enlarged crystal furnace no quantitative measure of crystal size nor the amount of residual anhydrous material that lay in the bottom of the column was made; it varied in depths from 10 to 20 cm. No gradual degradation of performance was observed by thermal cycling. The results of the data show a relatively constant heat storage capacity. Typical data for melt and freeze cycles are presented in Tables 3 and 4. Agreement between heat applied and heat withdrawn is shown in the tables to agree within about 2 percent of the two values measured experimentally.

The maximum heat extraction rate from the test container was approximately 23.5 kj/minute for a heat flow rate of about 16 $kwatts/m^2$. (See Figure 23.) This heat flow was determined to be about the maximum amount obtainable for the air flow rate used without causing crystal growth to form on the heat exchange tubing. Once the crystals formed on the heat exchange tubes, the heat flow rate was greatly reduced due to the thermal insulation of the immobile crystal structure attached to the heat exchange pipe. This pipe is approximately 1 cm in diameter and 317 cm long for a total heat exchange surface of 250 cm^2.

Some interesting observations can be drawn from the data of Tables 3 and 4. The theoretical amount of heat that should have been available between the temperatures indicated as stated previously was about 9700 kj. The actual amount of heat measured in Tables 3 and 4 and illustrated in Figure 23 is 4382 kj or only 45 percent of the theoretical value possible.

The two chief sources of this difference were probably due to the anhydrous salts that didn't take part in the fusion-melting process and in the heat leaks that exist through the walls of the container. Heat leaks do not necessarily represent wasted heat since the escaping heat can warm the surrounding medium in a beneficial way. The existence of anhydrous salt residue is undesirable, however. Since it neither absorbs nor gives up much heat it doesn't play a beneficial role in heat storage and it reduces heat storage capacity per unit volume of available storage space.

The enlarged 20 cm diameter crystal furnace was cycled ten times. During these ten cycles no progressive deterioration in heat storage capacity was discernible.

A problem arose with this unit that was not apparent in the smaller container. The air column was found to develop a preferred path through the anhydrous material that settles on the bottom of the container. It became apparent that either a small diameter salt container or else one which had tapered sides near the bottom was necessary. In this way salt can be funneled to the center where it will encounter the air column. A plastic funnel was placed at the bottom of the column giving the column bottom a 45° angle cone shape. This was found to function quite well although a steeper side would have functioned better.

Summary

Sodium sulfate decahydrate was selected as the most optimum material for heat storage. This decision was based on its latent heat of fusion (251 kj/kg) its melting point, good availability, and low cost (2-3 cents per pound, f.o.b. Great Salt Lake). Its thermal conductivity was also determined to be adequate provided crystal sizes were kept smaller, were fluidized, and were rapidly stirred. The melting point can be considered as both an advantage and as a disadvantage. One beneficial feature is that solar collectors are most efficient working where the heat sink is not at a very high temperature.

Several drawbacks to using Glauber salt were also recognized. The chief problem is a tendency for the salt crystals to decompose, losing the water molecule, and then settling out in an anhydrous form, rendering the crystals useless in the heat of fusion process. Another disadvantage is the fact that the latent heat is stored at 32.2°C which, after allowing for 2-3°C supercooling seriously limits the thermal gradient available across the heat exchanger. Large heat exchange surfaces and high velocity air currents are necessary to affect heat transfer as a result.

Table 3. Heat extracted from 23 liters of Glauber salt starting at an initial temperature of 34.4°C, with a final temperature of 24.1°C.

Time	Salt Temp °C	Water Temp Outlet	Water Temp Inlet	Change in Temp	Water Flow Rate ml/sec	Cal/min	BTU/min	Σ BTU	ΣK Joules
3:00 pm	34.4	21.1	12.2	8.9°C	20	10,680	42.4	0	0
3:10	31.1	19.4	11.9	7.8	16.7	7,816	31.	367	387
3:20	28.9	17.7	12.2	5.3	16.7	5,310	21.	627	661
3:30	28.3	16.7	11.1	5.6	16.7	5,611	22.3	843	889
3:40	28.3	16.7	11.1	5.6	16.7	5,611	22.3	1067	1127
3:55	28	16.7	12.2	4.3	16.7	4,309	17.1	1363	1438
4:05	27.8	17.8	12.2	5.6	16.7	5,611	22.3	1560	1646
4:15	27.8	17.8	12.2	5.6	16.7	5,611	22.3	1783	1881
4:25	27.8	17.5	12.2	5.3	16.7	5,310	21.	2000	2110
4:35	27.2	17.2	12.2	5.0	16.7	5,010	20.	2205	2326
4:45	27.2	17.2	12.2	5.0	16.7	5,010	20	2405	2537
4:55	26.9	17.2	12.2	5.0	16.7	5,010	20	2605	2748
5:10	26.7	17.2	12.2	5.0	16.7	5,010	20	2905	3065
5:20	26.4	15.6	12.8	2.8	16.7	2,806	11	3060	3228
5:30	26.1	15.6	12.2	3.4	16.7	3,407	13.5	3182	3357
5:40	26.1	15.6	12.2	3.3	16.7	3,306	13.1	3315	3497
5:50	26.1	14.4	11.1	3.3	16.7	3,306	13.1	3446	3635
6:00	25.8	13.9	11.1	2.8	16.7	2,807	11.1	3567	3763
6:10	25.6	14.4	11.7	2.8	16.7	2,807	11.1	3678	3880
6:20	25.6	14.4	12.2	2.2	16.7	2,204	8.7	3777	3985
6:30	25.3	13.9	12.2	1.7	16.7	1,703	6.8	3854	4066
6:40	25	13.9	12.2	1.7	16.7	1,703	6.8	3922	4138
6:50	24.7	13.9	12.2	1.7	16.7	1,703	6.8	3990	4209
7:00	24.4	14.4	12.2	2.2	16.7	2,204	8.7	4067	4291
7:10	24.1	14.4	12.2	2.2	16.7	2,204	8.7	4154	4382

Table 4. Heat absorbed by 23 liters of Glauber salt starting at an initial temperature of 23.3°C with a final temperature of 34.3°C.

Time	Salt Temp °C	Water Temp Outlet	Water Temp Inlet	Change in Temp	Water Flow Rate ml/sec	Cal/min	BTU/min	ΣBTU
1:30	23.3°C	36.7	44.4	7.8	27.8	13,010	51.6	-
1:40	25.5	37.2	47.8	10.6	27.8	17,681	70.2	609
1:45	25.8	38.9	51.1	12.2	27.8	20,349	80.7	986
1:50	26.7	39.4	53.9	14.5	27.8	24,186	96.0	1428
1:55	27.8	40.6	56.7	16.1	27.8	26,855	106.6	1930
2:00	28.9	41.1	58.9	17.8	27.8	29,690	117.8	2491
2:05	29.4	43.3	58.9	15.6	27.8	26,021	103.3	3044
2:10	31.1	45.6	60	14.4	27.8	24,019	95.3	3541
2:15	34.3	47.8	59.4	11.6	27.8	19,349	76.8	3971

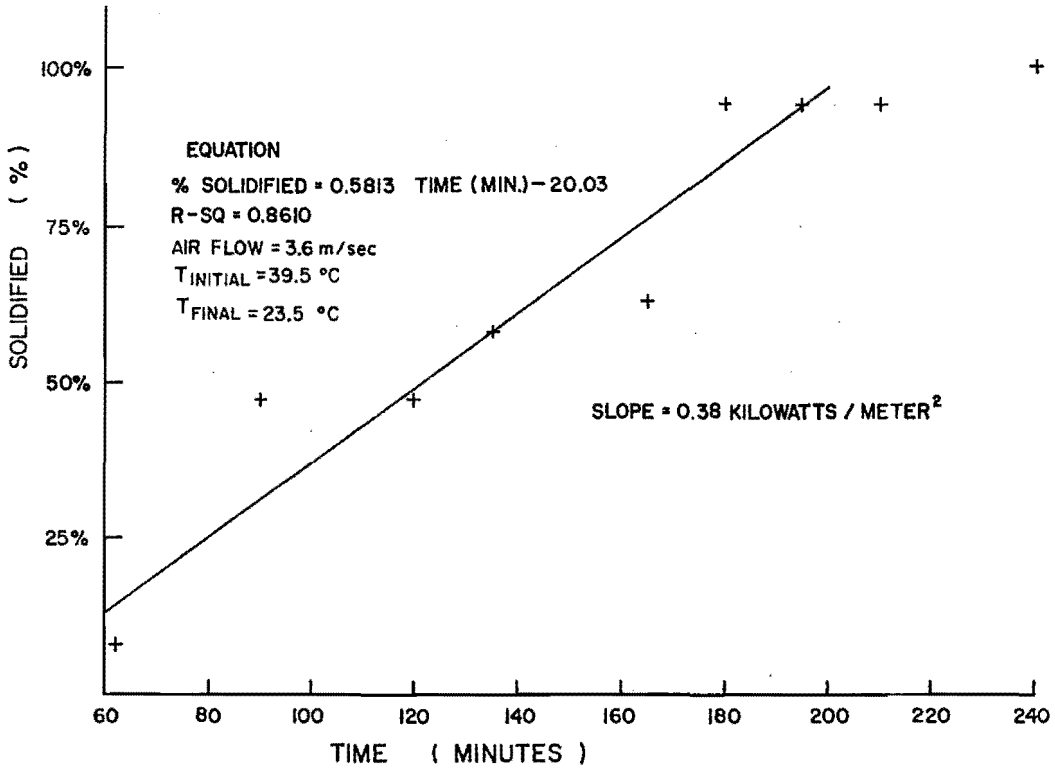

Figure 22. Heat release as a function of time in air stripped crystal furnace.

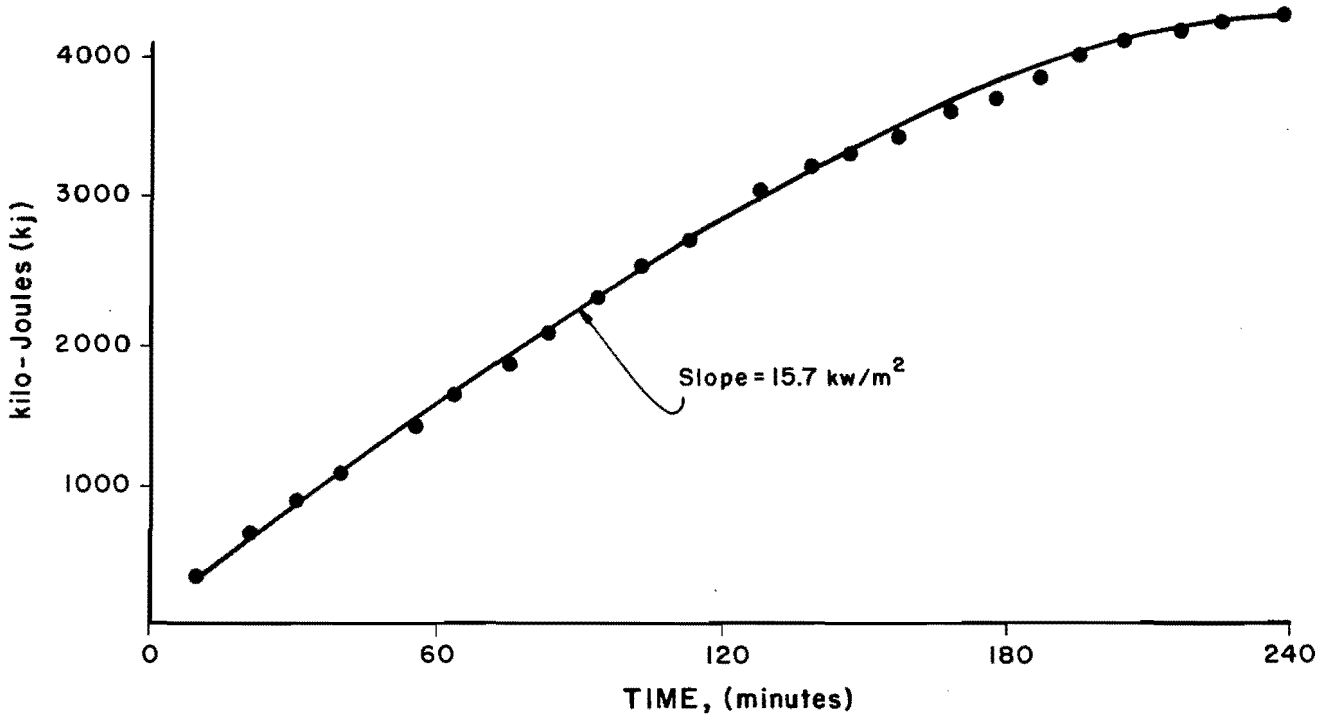

Figure 23. Heat release to heat pipes as a function of time in large air stirred crystal furnace. (Heat exchange tube has an area of 250 cm^2.)

Thickening Glauber salt greatly helps in preventing molecule separation, however its bulk cuts down the latent heat density almost by 50 percent which reduces by a factor of two the intrinsic heat storage advantage that unthickened salt theoretically possesses. The reduction of latent heat density in heavily thickened Glauber salt, coupled with the fact that only 40 to 60 percent of the theoretical heat possible was available after 1500 cycles, discouraged extensive study in plastic tube packaging. Two further comments on plastic packaging are worth noting, however. Thermal conductivity tests on the plastic tube packaged salt would indicate that heat flow is mainly limited by the thermal conductivity of the salt and not the plastic material. A suggested surface to volume ratio for the nearby free convective heat transfers coefficients, found to be most economical, is about 100 m^2/m^3.

The large heat transfer area requirement as determined in the report can be considerably reduced in containers internally stirred by aeration. This air stirred container serves both the purpose of increasing external/internal temperature gradients and allowing nearly complete reversal of the latent heat reactions without excessive anhydrous salt build-up.

Several problems were discovered during the operation of the aerated system. The chief problem is one of "channeling." Air escaping into the salt at the bottom of the salt container tends to rise to the surface in some preferred straight line path. For small diameter tubes of 10 cm or less, air injection salt mixing is quite adequate. If the diameter of the container is increased to about 25 cm the circulation becomes sluggish around the outside periphery under high-percentage crystal content conditions and some lodging of crystals near the bottom of the container occurs. The salt lodging at the bottom of the container is lost to the heat exchange-circulation process.

One method was discovered that worked quite well in alleviating the lack of adequate mixing at the bottom of the salt column. It consisted of making the bottom of the salt container cone shaped with the air jetting in at the center of the container and into the air stream. If a large container were to be used, multiple cones, and multiple air jets would have to be used. Attempts were made to send intermittent high pressure air jets to scour out the bottom of the salt column residue to eliminate the need for cones. This was not successful. The inertia of the air even at high velocity was so small compared to the inertia of the residue at rest that the air rose directly to the surface without accomplishing its intended purpose.

The other problem concerns the reliability of the air pump. As long as the pump functions properly, the system remains fluidized, and operational. If the air supply fails for any length of time, the entire system can freeze-up. Applying heat to thaw the entire mass without the aid of salt circulation is a slow process.

Possibilities of using Glauber salt in situations other than those discussed in this report are recognized. For example, Glauber salt could be placed inside overstuffed furniture. Such heat storage could easily double as a collector when placed in front of an undraped window, and as a radiator at night when the drapes are drawn. The feasibility of such alternative methods is considered to be beyond the scope of this report, however.

Conclusions

1. The high cost of commercially available thermal energy has impacted most of the homes in the United States.

2. The high energy density of the latent heat of fusion of Glauber salt ($Na_2SO_4 \cdot 10H_2O$) represents an alternative to water or rock sensible energy storage for temperatures under 150°C.

3. Much of the incongruent melting of Glauber salt ($Na_2SO_4 \cdot 10H_2O$) can be controlled by silica gel thickening or by stirring.

4. Thickening of Glauber salt ($Na_2SO_4 \cdot 10H_2O$) with silica gel reduces the realized latent heat by over 50 percent.

5. The thermal conductivity of silica gel thickened Glauber salt ($Na_2SO_4 \cdot 10H_2O$) is apparently quite variable, but averages about 0.61 watts/m°C.

6. Silica gel thickened Glauber salt ($Na_2SO_4 \cdot 10H_2O$) freezes with a nearly steady-state temperature profile in the solid phase.

7. Silica gel thickened Glauber salt ($Na_2SO_4 \cdot 10H_2O$) should not be packaged with surface area to volume ratios of less than about 100 m^2/m^3. This implies small thin packaging since a cubic has an area-volume ratio of only 6 m^2/m^3.

8. The cost of packaging thickened Glauber salt ($Na_2SO_4 \cdot 10H_2O$) with any packaging material costing more than about 20¢/m^2 leads to greater packaging cost than Glauber salt cost (1980 costs).

9. Glauber salt ($Na_2SO_4 \cdot 10H_2O$) energy storage using air stirring appears attractive if technical problems of air supply and container bottom configuration can be economically solved.

RECOMMENDATIONS FOR FUTURE RESEARCH

The possibility of finding a less expensive material than Glauber salt with higher latent heats of fusion appears doubtful. The possibility of recovering the full latent heat of thickened Glauber salt may ultimately be possible. Perhaps a slightly higher water and gel content than that stoichiometrically required would increase diffusion in the gel as crystallization occurs. An improvement in the thermal conductivity of thickened Glauber salt would certainly save considerable money spent on packaging. It should be remembered, however, that thin packaging with the large dimension being in the horizontal placement is at present extremely important to reducing degradation.

Exclusive of the solar collectors, the largest cost seems to be for the packaging and/or container. An inexpensive surfacing material could reduce costs a great deal. The long-term durability of 10 mil polyethylene needs more extensive study. A less expensive material than polyethylene does not seem to be available.

Air stirred crystallization seems a promising approach. If the container configuration and air pump supply problems can be overcome, considerable money can be saved by this approach. The pressures necessary to maintain stirring are nominal, as are the volumetric flow rates required. The heat transfer from the crystallizing liquid is very favorable. The second major advantage of stirring is the high reversibility and therefore high realized latent heat for stirred Glauber salt.

Other promising applications of Glauber salt appear to be those involving architectural and structural packaging. Ceiling tiles have been explored by Johnson (1977). Wall paneling is another possibility, but long vertical containers can cause a separation problem. Floor tiles offer a good possibility of high heat transfer coefficients, but may represent a puncture problem. A potentially very marketable product might be furniture with Glauber salt included in construction. Air duct work could easily be designed with Glauber salt included. Such a heating system would of necessity require careful engineering to avoid storing expensive auxiliary heat.

LITERATURE CITED

Altman, M. 1971. Conservation and better utilization of electric power by means of thermal energy storage and solar heating. Technical Report No. PB-210 359. Towne School of Civil and Mechanical Engineering. October 1971. NSF-GI 279 76.

APHA. 1975. Standard methods for the examination of water and wastewater. 14th Ed. Prepared jointly by APHA, AWWA, and WPCF.

Bauerle, G., D. Chung, G. Ervin, J. Guon, and T. Springer. 1975. Storage of solar energy by inorganic oxide/hydroxides. Report for Atomics International Division Rockwell International, 27 p. NSF Grant AER 74-09069.

Biswas, D. R. 1977. Thermal energy storage using sodium sulfate decahydrate and water. Solar Energy 19:99-100.

Carslaw, H. S., and J. C. Jaeger. 1959. Conduction of heat in solids. Oxford Univ. at the Clarendon Press, London. 510 p.

Colloidal Materials. 1979. Personal communication, Sheet 617-475-3276. P.O. Box 696, Andover, MA 01810.

Ernst Home Center. 1980. Personal communication.

Findlay, A. 1945. The phase rule. 8th Ed. Dover Publications, New York. 252 p.

Great Salt Lake Mineral Co. 1980. Personal communication.

Hashemi, H. T., and C. M. Sliepcevich. 1967. A diffusion analogue method for solving problems of heat conduction with change of phase. Heat Transfer with Phase Change. 63(79):1-85. A Chemical Engineering Progress Symposium Series, published by American Institute of Chemical Engineers.

Henisch, H. K. 1970. Crystal growth in gels. Pennsylvania State University Press, University Park, PA. 111 p.

Herrick, C. S., and R. F. Thornton. 1979. Rolling cylinder thermal storage. Thermal Energy Storage Subsystems for Solar Heating and Cooling Applications - (Interim Report), prepared under contract DE-AC05-780R05759 SRD-79-089, General Electric. pp. 1.0-1 to 5.0-1.

Holman, J. P. 1966. Experimental methods for engineers. McGraw-Hill Book Co., Inc., New York. 412 p.

Holman, J. P. 1972. Heat transfer. McGraw-Hill Book Co., Inc., New York. 462 p.

Hottel, H. C., and J. B. Howard. 1971. New energy technology - some facts and assessments. M.I.T. Press, Boston.

Johnson, T. E. 1977. Lightweight thermal storage for solar heated buildings. Solar Energy 19:669-675.

Jurinak, J. J., and S. I. Abdel-Khalik. 1978. Properties optimization for phase-change energy storage in air-based solar heating systems. Solar Energy 21:377-383.

Keller, L. 1978. A new type of thermal phase-change storage. Solar Energy 21:449.

Lane, G. A., D. N. Glew, E. C. Clarke, S. W. Quigley, and H. E. Rossow. 1975a. Isothermal solar heat storage materials, phase I. Technical Report, Sept. 1974 to April 1975. ERDA-117 UC 942 Contract NSF-C906.

Lane, G. A., J. S. Best, E. C. Clarke, D. N. Glew, G. C. Karris, S. W. Quigley, and H. E. Rossow. 1975b. Solar energy subsystems employing isothermal heat sink materials. Semi-annual Progress Report, Sept. 18, 1974-June 31, 1975. Contract NSF-C906.

Lane, G. A., J. S. Best, E. C. Clarke, S. S. Drake, D. N. Glew, S. W. Quigley, and H. E. Rossow. 1975c. Solar energy subsystems employing isothermal heat sink materials. Semi-annual Progress Report, Sept. 18, 1974-June 31, 1975. NSF Contract NSF-C906, PB-246-342.

Lane, G. A., J. S. Best, E. C. Clarke, D. N. Glew, G. C. Karris, S. W. Quigley, and H. E. Rossow. 1976. Solar energy subsystems employing isothermal heat sink materials. Final Report, Sept. 18, 1974-March 18, 1976. NSF Contract NSF-C906. NTIS. 15 p.

Lefrois, R. J., G. R. Knowles, A. K. Mathur, and J. Budimir. 1979. Active heat exchange system development for latent heat thermal energy storage. pp. 1-1, 5-25. Prepared under Contract DEN 3-38 DOE/NASA/0038-79/1 NASA CR 159479 HI#79063 Order #N79-21554.

Lorsch, H. G. 1974. Thermal energy storage devices suitable for solar heating. 9th Intersociety Energy Conversion Engineering Conference Proceedings. American Society of Mechanical Engineers Publication. New York.

Mills, A. D., S. S. Melsheirmer, and D. D. Edie. 1979. Extended cycling behavior of a direct contact - phase change TES system. 72nd Annual AlChE Meeting. San Francisco, CA. 23 p.

Montillion, G. H., and W. L. Badger. 1927. Rate of growth of crystals in aqueous solutions. Industrial and Engineering Chemistry 19(7):809-816.

Morrison, D. J., and S. I. Abdel-Khalik. 1978. Effects of phase-change energy storage on the performance of air-based and liquid-based solar heating systems. Solar Energy 20:57-67.

Obert, E. F., and R. L. Young. 1962. Elements of thermodynamics and heat transfer. 2nd Ed. McGraw-Hill Book Co., Inc., New York. 537 p.

Prengle, H. W., and C. H. Sun. 1976. Operational chemical storage cycles for utilization of solar energy to produce heat or electric power. Solar Energy 18:561-567.

Ratcliffe, E. H. 1968. Thermal conductivities of two-phase media: Methodology, results, estimations. Thermal Conductivity Proceedings of the 8th Conference. Purdue Univ., Plenum Press, NY, pp. 1141-1147.

Samons, Home Improvement. 1980. Personal communication.

Schmidt, E. W., and P. A. Lowe. 1976. Thermochemical energy storage systems. 11th Intersociety Energy Conversion Engineering Conference Proceedings. American Society of Mechanical Engineers Publication. New York.

Shaffer, L. H. 1978. Viscosity stabilized solar ponds. Sun-Mankind's Future Source of Energy. Proceedings of the International Solar Energy Society, 2:1171-1175. Pergamon Press, New York.

Sharp, M. K., and R. I. Loehrke. 1979. Stratified versus well-mixed sensible heat storage in a solar space heating application. ASME Publication #78-HT-49. 7 p.

Solar, Inc. 1977. Heat storage tray. Engineering Data Sheet #200.

Telkes, M. 1974. Solar energy storage. ASHRAE Journal, Sept. 1974, pp. 38-44.

U.S. Dept. of Labor. 1980. Monthly labor review, March 1972 to Feb. 1980. U.S. Government Printing Office, Washington, D.C.

Washburn, E. W. (Ed.). 1929. International critical tables. International Research Council and National Academy of Science, by National Research Council of U.S.A. McGraw-Hill Book Co., Inc., New York.

APPENDIX A

THERMAL CONDUCTIVITY OF TWO PHASE MEDIA

The thermal conductivity of two phase media such as Glauber salt in a near liquid gel is a complex problem. Ratcliffe (1968) has presented a nomograph for estimating thermal conductivity in two phase media. Figure 4 shows extensive variability in the measured thermal conductivity for thickened Glauber salt even when internal temperatures are repeated. The mean value was about 0.61 watts/m°C. This is in good agreement with the expectation from Ratcliffe's nomograph that the thermal conductivity of the continuous portion will determine the central tendency of the combined thermal conductance. The thermal conductivity of water at 20°-25°C is between 0.60 and 0.62 watts/m°C.

The solidification process in a gel is discussed at length by Henisch (1970). Diffusion can slow crystal growth a great deal in gelled suspensions. This could possibly lead to a time dependent water content in the continuous phase. The effect of a slow dehydration on thermal conductivity is not known.

The contraction of paraffin wax was observed to generate cavities in the wax. It is very possible that micro-cavities form in thickened Glauber salt as Jurinak and Abdel-Khalik (1978) report the density of Glauber salt changes from 1460 kg/m^3 in the solid state to 1330 kg/m^3 in the liquid state. No such 9 percent volume change was observed with thickened material. Settling or rapid freezing could well produce small cavities which insulate against heat transport. The size of the crystals formed is very definitely strongly dependent on the rate of crystallization. Rapid cooling leads to small crystals. It is of interest that the most rapidly frozen material studied produced a very low thermal conductivity.

Of particular interest is the maintenance of a high thermal conductivity when large amounts of the Glauber salt were melted out. This is another indication of the importance of the continuous media in determining the overall thermal conductivity of the material. It should be indicated in this discussion of these losses of Glauber salt that the great majority of the material melted out saturated the urethane foam at the bottom increasing conductance through the bottom of the apparatus.

APPENDIX B

SYMBOLS, ABBREVIATIONS, DIMENSIONS, AND UNITS

Symbols and Abbreviations

A = the area of something (L^2)

a = the radius of a heat storage material container (L)

C = the specific heat of something (E/MT)

C_{air} = the specific heat of air (E/MT)

C_{Gl} = the specific heat of Glauber salt (E/MT)

C'_{Gl} = the specific heat averaged with the latent heat of Glauber salt (E/MT)

C_{wa} = the specific heat of water (E/MT)

C_1 = a proportionality constant relating crystal surface to time of crystallization (L^2/t)

C_2 = a proportionality constant

C_3 = an exponential multiplier for base e for determining weight to surface relations in crystal growth (M/L^2)

C_4 = an exponentiation constant for determining weight to surface relations in crystal growth ($1/t$)

d = the diameter of something (L)

F = the geometric view factor for radiation heat transfer (dimensionless)

g = the acceleration caused by the gravitional force (9.81 m/sec^2)

H = the latent heat of a phase change energy storage material (E/M)

h = heat transfer coefficient (E/L^2Tt)

k = the thermal conductivity of something (E/LTt)

k_f = the thermal conductivity of air (E/LTt)

k_L = the thermal conductivity of liquid material (E/LTt)

k_s = the thermal conductivity of solidified material (E/LTt)

ℓ = the length of sections of tubing in a heat exchange array (L)

L = the total length of something (L)

n = the number of tubes in a heat exchange array (dimensionless)

q = the heat transfer rate (E/t)

$\dot{q}$ = the heat generated per unit volume per unit time (E/L^3t)

Q = absolute amount of heat (E)

Ra = Rayleigh dimensionless group

Re = Reynolds dimensionless group

r = the radius of something with circular geometry (L)

r_{crit} = the critical radius (L)

r_i = the inside radius (L)

r_o = the outside radius (L)

R_o = the outside radius of the annulus of material in the thermal conductivity apparatus (L)

R_i = the inside radius of the annulus of material in the thermal conductivity apparatus (L)

s = the spacing between adjacent tubes in a heat exchange (L)

S = the surface area of a growing group of crystals (L^2)

T = the temperature of something (T)

T_{bulk} = the deep bulk mid-stream temperature (T)

T_{eq} = the final equilibrium temperature with entropy maximized (T)

T_{exit} = the temperature of the air at the exit (T)

T_{ext} = the temperature at the exterior surface of the latent heat energy storage material (T)

T_h = higher temperature (T)

T_{Gl} = the temperature of the Glauber salt (T)

T_{inlet} = the temperature of the air at the inlet (T)

T_o = initial temperature (T)

T_{melt} = the melting or phase change temperature (T)

T_{wall} = the wall temperature of a body (T)

T_{wa} = the temperature of water (T)

v = value of a heat storage material (E/$)

V = volume of something (L^3)

$\dot{V}$ = volumetric flow rate = V/τ (L^3/t)

W = weight gained by a group of growing crystals (M)

$\bar{y}$ = a characteristic depth in the Rayleigh number (L)

$ = the cost of something ($)

α = the thermal diffusivity (L^2/t)

β = the coefficient of volumetric expansion (dimensionless)

∂ = the partial of a variable for partial differentiation (i.e., $\partial R/\partial \tau$)

ε = the emissivity of a gray body radiator (dimensionless)

π = 3.1415, the ratio of the circumference to the diameter of a circle

ρ = density of something (M/L^3)

ρ_{air} = density of air (M/L^3)

ρ_{Gl} = density of Glauber salt (M/L^3)

ρ_{wa} = density of water (M/L^3)

σ = the Stefan-Boltzmann constant - 5.6697×10^{-8} $W/m^2{}^oK^4$ (E/T^4L^2t)

μ_∞ = the free or midstream velocity of air (L/t)

γ = the kinematic viscosity (L^2/t)

γ_f = the kinematic viscosity of air (L^2/t)

τ = time (t)

Dimensions

E = energy (cal., Joules, kilojoules)

L = length (kilometers, meters, cm, mm, or nm)

M = mass (kg or grams)

t = time (days, hours, min, sec)

T = temperature (^oC, ^oK)

$ = money ($ or ¢)

Units

cm = centimeters

g = grams

J = Joules

kg = kilograms

kJ = kilojoules

kW = kilowatts

kWhr = kilowatt-hours

m = meters

sec = seconds

W = watts